Biotechnology Advances

Overview of Flavin-containing Monooxygenase: History, Structures, Mechanism, Biosynthesis and Disease

--Manuscript Draft--

Manuscript Number:	JBA-D-23-00665
Article Type:	Review Article
Keywords:	Flavin-containing Monooxygenase, Synthetic Biology, Catalytic Mechanism, Indigo and indirubin biosynthesis, Bio-indigo
Corresponding Author:	Yunjun Yan Wuhan, Hubei CHINA
First Author:	Changxin Fan
Order of Authors:	Changxin Fan
	Ziqi Xie
	Yijin Li
	Ruihan Zhang
	Da Zheng
	Jiacheng Shi
	Yifei Wang
	Mingyuan Cheng
	Yu Zhou
	Yi Zhan
	Yunjun Yan
Abstract:	The Flavin-containing Monooxygenases (FMOs) are a significant protein family that is widely distributed in bacteria, yeasts, plants, and mammals. FMOs have been demonstrated to play a crucial functional role in drug metabolism and indigo biosynthesis. The research history of FMOs was reviewed. The structural analysis of FMOs was conducted to point out the catalytic mechanism, which can aid in comprehending their functions more profoundly. The catalytic example of indole was exhibited in the docking simulation. The differences across FMOs were comprehensible among sequence alignments. The potential improvements of FMOs were provided through de novo design, directed evolution, enzyme immobilization, metabolic engineering, and fermentation engineering, which provides additional insights into indigo and indirubin biosynthesis via FMOs.
Suggested Reviewers:	Pablo Sobrado, PhD Professor, Virginia Polytechnic Institute and State University University Bookstore psobrado@vt.edu Their group studied the mechanism of mFMO and found that tryptophan-47 is important.
	Andrea Mattevi, PhD Professor, University of Pavia mattevi@ipvgen.unipv.it They solved the structure of mFMO.
	Si Wouk Kim, PhD Professor, Chosun University swkim@chosun.ac.kr The first group applied mFMO in indigo biosynthesis.
	Marco W. Fraaije, PhD Professor, University of Groningen

Powered by Editorial Manager® and ProduXion Manager® from Aries Systems Corporation

	m.w.fraaije@rug.nl They achieved the highest yield of indigo biosynthesis so far.
	Jin Ho Lee, PhD Professor, Kyungsung University jhlee83@ks.ac.kr They cloned cFMO from Corynebacterium glutamicum to improve the yield of indigo and indirubin.
	Gui Hwan Han, PhD Professor, Center for Industrialization of Agricultural and Livestock Microorganisms ghhan@cialm.or.kr Great works in indigo biosynthesis
	Yung Hun Yang, PhD Professor, Konkuk University seokor@konkuk.ac.kr This group recently utilized some new strategies to improve the yield of bio-indigo.
	Byung Gee Kim, PhD Professor, Seoul National University byungkim@snu.ac.kr FMO was used to synthesize tyrian purple. A consecutive two-cell reaction system was used.
	Feng-Qing Wang, PhD Professor, East China University of Science and Technology fqwang@ecust.edu.cn They engineered bFMO for the efficient production of indirubin

Powered by Editorial Manager® and ProduXion Manager® from Aries Systems Corporation

COVER LETTER

Yunjun Yan
College of Life Science and Technology, HUST
1037 Luoyu Road, Hongshan District, Wuhan 430074, P.R. China.

Submission date:
September 20, 2023

Edward A. Bayer
Weizmann Institute of Science, Department of Biomolecular Sciences, Rehovot, Israel

Dear Prof. Edward A. Bayer,

We are pleased to submit our manuscript entitled "Overview of Flavin-containing Monooxygenase: History, Structures, Mechanism, Biosynthesis and Disease" for full consideration as an original article to the Journal "*Biotechnology Advances"*. This review totally investigated the research history, structures, mechanisms, and potential improvements of flavin-containing monooxygenase (FMO), specially focusing on how to improve the biosynthesis of indole and indirubin. We know the aims and scope of *Biotechnology Advances* are on current developments and future trends in biotechnology. Our review exhibits the potential application of FMOs in the industry and includes the research history and future developing trends in improving the biosynthesis of indigo and indirubin via FMOs from various aspects. We believe this article will be of special interest to the readers of *Biotechnology Advances*.

This manuscript has not been previously published and is not under consideration in the same or substantially similar form in any other peer-reviewed media.

AUTHOR INFORMATION

Corresponding Authors

Yunjun Yan - Key Laboratory of Molecular Biophysics of the Ministry of Education,

Huazhong University of Science and Technology, 430074 Wuhan, People's Republic of China

Email: *yanyunjun@hust.edu.cn*

Yi Zhan - College of Life Science and Technology, Huazhong University of Science and Technology, 430074 Wuhan, People's Republic of China

Email: *zhanyi@hust.edu.cn*

Yu Zhou - College of Life Science and Technology, Huazhong University of Science and Technology, 430074 Wuhan, People's Republic of China

Email: *zhoyu@hust.edu.cn*

Authors

Changxin Fan - College of Life Science and Technology, Huazhong University of Science and Technology, 430074 Wuhan, People's Republic of China

orcid.org/0000-0002-0435-6202; Email: *cfanai@connect.ust.hk*

Ziqi Xie - College of Life Science and Technology, Huazhong University of Science and Technology, 430074 Wuhan, People's Republic of China

orcid.org/0000-0001-8435-1948; Email: *ziqi_xie@hust.edu.cn*

Yijin Li - Innovation Base of Life Science and Technology, Qiming College, Huazhong University of Science and Technology, 430074 Wuhan, People's Republic of China

Email: *u202013531@hust.edu.cn*

Ruihan Zhang - College of Life Science and Technology, Huazhong University of Science and Technology, 430074 Wuhan, People's Republic of China

Email: *peterico3395@163.com*

Da Zheng - College of Life Science and Technology, Huazhong University of Science and Technology, 430074 Wuhan, People's Republic of China

Email: *zhengnda@outlook.com*

Jiacheng Shi - College of Life Science and Technology, Huazhong University of Science and Technology, 430074 Wuhan, People's Republic of China

Email: *shijiachengg@163.com*

Yifei Wang - Innovation Base of Life Science and Technology, Qiming College, Huazhong University of Science and Technology, 430074 Wuhan, People's Republic of China

Email: *wang.ef@foxmail.com*

Mingyuan Cheng - College of Life Science and Technology, Huazhong University of Science and Technology, 430074 Wuhan, People's Republic of China

Email: *chengmingyuann@163.com*

CRediT authorship contribution statement

Changxin Fan: Conceptualization, Formal analysis, Investigation, Writing - Original Draft, Writing - Review & Editing, Visualization. **Ziqi Xie**: Conceptualization, Investigation, Writing - Original Draft, Writing - Review & Editing, Visualization. **Yijin Li**: Investigation, Writing - Original Draft, Visualization. **Ruihan Zhang**: Investigation, Writing - Original Draft. **Da Zheng**: Formal analysis, Investigation, Writing - Original Draft, Visualization. **Jiacheng Shi**: Investigation, Writing - Original Draft. **Yifei Wang**: Investigation, Writing - Original Draft. **Mingyuan Cheng**: Visualization. **Yu Zhou**: Supervision. **Yi Zhan**: Supervision, Project administration, Writing - Original Draft. **Yunjun Yan**: Project administration, Writing - Review & Editing, Funding acquisition.

Conflict of interest

The authors declare no financial or commercial conflict of interest.

I appreciate your consideration of this manuscript.

Sincerely,

Yunjun Yan

Declaration of interests

☒The authors declare that they have no known competing financial interests or personal relationships that could have appeared to influence the work reported in this paper.

☐The authors declare the following financial interests/personal relationships which may be considered as potential competing interests:

Highlights

- Flavin-containing monooxygenases (FMOs) have been involved in indigo biosynthesis for over 20 years.
- The relationship between structure and catalytic mechanism of flavin-containing monooxygenases is elucidated.
- Directed evolution, *de novo* design, and genome-scale metabolic network models (GEMs) are suggested to improve indigo and indirubin biosynthesis.
- Trimethylaminuria (TMAU) is a genetic disorder caused by a defect in hFMO3.

Manuscript Click here to view linked References

Overview of Flavin-containing Monooxygenase: History, Structures, Mechanism, Biosynthesis and Disease

Changxin Fan[a,b,1,2], Ziqi Xie[a,b,2], Yijin Li[b,2], Ruihan Zhang[a,b,2], Da Zheng[a,b,2], Jiacheng Shi[a,b], Yifei Wang[b], Mingyuan Cheng[a,b], Yu Zhou[a,c,*], Yi Zhan[a,c,*], Yunjun Yan[a,c,*]

[a] *College of Life Science and Technology, Huazhong University of Science and Technology, Wuhan 430074, People's Republic of China*

[b] *Innovation Base of Life Science and Technology, Qiming College, Huazhong University of Science and Technology, Wuhan 430074, People's Republic of China*

[c] *Key Laboratory of Molecular Biophysics of the Ministry of Education, Huazhong University of Science and Technology, Wuhan 430074, People's Republic of China*

[1] Present address: Division of Life Science, HKUST, Clear Water Bay, Kowloon, Hong Kong, P.R.China.

[2] These authors contributed equally to this work.

[*] Corresponding author at: College of Life Sciences and Technology, Huazhong University of Science and Technology, 1037#, Luoyu Road, Hongshan District, Wuhan 430074, P.R. China.

E-mail address: yanyunjun@hust.edu.cn (Y. Yan).
zhanyi@hust.edu.cn (Y. Zhan).
zhoyu@hust.edu.cn (Y. Zhou).

Abstract

The Flavin-containing Monooxygenases (FMOs) are a significant protein family that is widely distributed in bacteria, yeasts, plants, and mammals. FMOs have been demonstrated to play a crucial functional role in drug metabolism and indigo biosynthesis. The research history of FMOs was reviewed. The structural analysis of FMOs was conducted to point out the catalytic mechanism, which can aid in comprehending their functions more profoundly. The catalytic example of indole was exhibited in the docking simulation. The differences across FMOs were comprehensible among sequence alignments. The potential improvements of FMOs were provided through *de novo* design, directed evolution, enzyme immobilization, metabolic engineering, and fermentation engineering, which provides additional insights into indigo and indirubin biosynthesis via FMOs.

Keywords: Flavin-containing Monooxygenase, Synthetic Biology, Catalytic Mechanism, Indigo and indirubin biosynthesis, Bio-indigo

Contents

Introduction

In 2006, flavoprotein monooxygenases (FPMOs) were classified into six classes according to sequence and structure date (van Berkel et al., 2006). Flavin-containing Monooxygenase (FMO, EC 1.14.13.8) belongs to class B, which is encoded by a single gene and contains a tightly bound FAD cofactor. FMO retains the coenzyme NADPH/$NADP^+$ bound during catalysis and is composed of two dinucleotide binding domains (Rossmann fold) that bind FAD and NADPH, respectively. Recently, it was discovered that FMO can be classified into two subtypes: type I and type II (Jensen et al., 2012; Riebel et al., 2013). Type I FMOs depend on NADPH as the coenzyme, which are discussed mainly in this paper. While type II FMOs, such as *Stenotrophomonas maltophilia* flavin-containing monooxygenase (SMFMO), which can perform Baeyer–Villiger oxidation and accept both NADPH and NADH as coenzymes, have not been extensively studied (Ceccoli et al., 2014).

Eukaryotic FMOs are widely present in the livers of *Oryctolagus cuniculus*, *Sus scrofa*, and *Homo sapiens* and are located at the endoplasmic reticulum (ER) of hepatocytes towards the cytoplasm. Similar to cytochrome P450 (CYP450), FMOs are involved in drug metabolism and mono-oxidation N and S of xenobiotic compounds. Human FMO is classified into five categories: hFMO1, hFMO2, hFMO3, hFMO4, and hFMO5. Studies on FMO1 in pig livers, the former hotspot in the related area, have revealed the catalytic mechanism and the universality of substrates of FMOs (Table 2)

(Poulsen and Ziegler, 1979; Ball and Bruice, 1980; Beaty and Ballou, 1981a, b; Ziegler, 1993). The expression levels of FMOs vary significantly across different species (Table 1). The species specificity of FMO is likely relevant to the susceptibility and secretion efficiency of toxins and xenobiotics. Furthermore, even within humans, the expression levels of hFMOs can vary depending on factors such as tissue, age, and sex (Zane et al., 2018). hFMO1 exists mainly in fetal livers, adult kidneys, and intestines, while hFMO3 is mainly expressed in adult kidneys. hFMO3, owing to its significance in disease, is currently the most extensively studied (Phillips and Shephard, 2020a). It was found that a close link between hFMO3 mutation and trimethylaminuria (TMAU) (Treacy et al., 1998).

Unlike mammals, yeast only has one FMO isoform, yFMO, which exerts its effect on protein folding (Suh et al., 1996; Suh et al., 1999). In plants, FMO is the rate-limiting enzyme in auxin biosynthesis, catalyzing oxidative decarboxylation of indole-3-pyruvate acid (IPyA) to form indole-3-acetic acid (IAA) (Cao et al., 2019). Bacterial FMO, also known as trimethylamine monooxygenase (TMM), besides oxidizing many compounds containing nitrogen and sulfur, is also able to oxidize indole, trimethylamine (TMA), dimethylsulfate (DMS), and dimethylsulfoxide (DMSO) (Chen et al., 2011; Choi et al., 2003). Through metagenomes, TMM was found to play a pivotal but often neglected role in the global carbon and nitrogen cycles (Chen et al., 2011). The first bacterial FMO, *Methylophaga* sp. strain SK1 (mFMO) (Choi et al.,

2003), was used in engineered *Escherichia coli* to produce indigo. Further research suggested that it also catalyzes indole derivatives into indigoid dyes (Rioz-Martinez et al., 2011). It is important to note the mechanism of FMOs in the synthesis of indigo. In bacteria, tryptophan is converted to indole by tryptophanase (TRP), and FMOs subsequently oxidize indole to 2-hydroxyindole or 3-hydroxyindole, which are oxidized to isatin by oxygen. Isatins then dimerize into indigo or indirubin (Fig. 5C).

Indigo, a natural dye commonly extracted from plants, has a history of over 6,000 years of traditional extraction techniques. Indigo is widely used in the textile industry for dyeing jeans and other fabrics. However, the production of around 80,000 tonnes of indigo each year involves the use of non-renewable petrochemicals and results in the generation of toxic compounds (Linke, J.A. et al., 2023). To address these issues, bio-indigo, which involves the use of synthetic biology to synthesize indigo from tryptophan or indole, has been proposed as a sustainable and eco-friendly alternative. Although several countries, such as China, America, and France, have companies that are making efforts to commercialize bio-indigo, the process has been hindered by low yields. FMOs, which have been shown to possess the ability to synthesize bio-indigo, are regarded as promising enzymes to overcome this limitation. Indirubin, an indole alkaloid used as a drug in chronic myeloid leukemia, has shown anticancer effects (Yang et al., 2022), and traditional production methods rely on plant cell culture extraction (Han et al., 2012). Biosynthetic processes are needed to improve production

efficiency and conditions (Berry et al., 2002; Choi et al., 2003; Cho et al., 2011).

Except biosynthesis, FMOs also play crucial roles in other aspects. The superoxide anion radical generated by FMOs is considered to regulate the overall redox state of cells (Krueger and Williams, 2005). In *Caenorhabditis elegans*, *fmo-2/FMO5* is regulated by NHR-49/PPAR-a during infection of *Staphylococcus aureus*, revealing that FMOs are critical innate immunity effectors in animals (Wani et al., 2021). In mice, the biological clock genes regulate FMO5 expression by transcription of cis-acting elements E-box and D-box (Chen et al., 2019), suggesting that hFMOs may play a more extensive role in the human body.

This paper provides a comprehensive review of the research progress on FMOs, particularly on mFMO. The structure and catalytic mechanism of mFMO are highlighted, and the advances in indigo and indirubin biosynthesis are discussed, providing a prospect for scientists to improve the yields through new strategies and potentially expand the application of mFMO.

1. The research history of FMOs

1.1 The evolution and diversity of the FMO gene family

In 1972, Dr. Ziegler isolated a mixed-function enzyme from the pig liver that catalyzes N-oxidation of amine (Fig. 1) (Ziegler and Mitchell, 1972). The enzyme can oxidize a wide variety of nitrogen-, sulfur-, and phosphorus-containing xenobiotics. It was named

Flavin-containing Monooxygenases, rather than being named restrictively mixed-function, amine oxidase, or simply N-oxidase (Ziegler, 2002).

----------**Fig 1**----------

In the 1980s, Tynes et al. identified differences between hepatic and pulmonary forms of microsomal FMO in mice and rabbits (Tynes et al., 1985). Since then, over 150 types of FMOs have been successfully isolated from various species (van Berkel et al., 2006). Currently, there are 11 genes encoding hFMOs in *H. sapiens* (*FMO1-FMO5*, *FMO6P-FMO11P*), of which only *FMO1-FMO5* encode catalytic proteins. FMO 1-5 share approximately 50%-58% amino acid identity across different species (Lawton et al., 1994; Yang, 2017).

The FMO gene family is conserved across all phyla that have been examined so far. Hence, some forms of the FMO gene family can be found in all studied eukaryotes. FMO genes are defined by specific structural and functional restrictions, which have prompted the evolution of different types of FMOs to fulfill various tasks. The functional subtypes of FMOs (FMO 1-5) began to diverge before the evolution of mammals and amphibians into distinct classes. FMO5, which was identified in vertebrates, is the first functionally unique member of the FMO family and appears to have evolved earlier than other forms of FMOs. According to phylogenetic studies, the

most recent FMOs to develop into enzymes with distinct functions are FMO1 and FMO3. FMOs in invertebrates have developed polyphyletically, which means that an invertebrate evolved a phenotypically similar gene that was not passed down from a shared ancestor (Hao et al., 2009).

FMO proteins share several conserved domains are shown in Figure 2, including the FAD binding domain (GxGxxG/A) (Burnett et al., 1994), the FMO protein recognition motif (FxGxxxHxxxY/F) (Alfieri et al., 2008), and the $NADP^+$ binding domain (GxSxxG/A) (Lawton et al., 1994). Leu375 is conserved in both hFMO and AncFMO (ancient mammalian FMO), and acts as a tunnel gatekeeper (Levin, 1992). Asn78 in mFMO is conserved in all FMOs (marked green in Fig. 5), and two additional oxygen molecules are located in its side chain group, contributing to the stability of oxygen molecules through polarity and affecting enzyme activity in various FMO proteins (Alfieri et al., 2008).

It is worth noting that while hFMO is an insoluble protein, mFMO is water-soluble and its FAD is exposed to the solvent, making it easier to bind to the matrix (Phillips and Shephard, 2020b). The homology between the two proteins is only 20.7% (Fig. 2B). Furthermore, as shown in Fig. 2B, cFMO, cloned from *Corynebacterium glutamicum*, has little homology with various FMO proteins found in bacteria and mammals.

----------Fig 2----------

181

182 **Table 1**. The expression difference of mammalian FMOs

Species	FMO subtypes	Tissue	Developmental stage	Sex difference	References
Homo sapiens	FMO1	-The primary subtype in adult kidney	-High expression in fetal, silent post parturition	-No significant gender difference	Dolphin et al., 1996; Hernandez et al., 2004; Zhang and Cashman, 2006
	FMO2	-The primary subtype in *adult* lung			
	FMO3	-The primary subtype in adult liver	-Low expression in fetal, gradually increases post parturition		
	FMO4	-Liver, kidney, lung, small intestine et al.			
	FMO5	-Liver, small intestine, kidney, lung et al.			
Mus musculus	FMO1	-Lung, kidney, brain	-Expression in fetal liver gradually increased to reach that of female mice levels post parturition; Expression in the brain is the most in neonatal	-Gender difference is noticeable 28 days after birth. The expression in female mice remains unchanged, while that of male mice is inhibited	Cherrington et al., 1998; Janmohamed et al., 2004
	FMO2	- Low expression		-No significant gender difference	
	FMO3	-The primary subtype in adult female mouse liver	-Fetal liver expression is low and reaches adult expression level 14 days post parturition	-Gender differences demonstrated after sexual maturity	
	FMO4	-Low expression		-No obvious	

				gender difference	
	FMO5	-Liver, kidney, small intestine	-Expression is detectable 17 days after gestation and reaches the expression of adult level 2 days post parturition	-Expression level in female mice was higher than that of male mice in liver and kidney	
Rattus norvegicus	FMO1	-Liver		-Higher expression level in males than female	Cherrington et al., 1998; Lattard et al., 2003
	FMO2	-Kidney		-No obvious gender difference	
	FMO3	-Liver (lower expression level than that of FMO1)			
	FMO4	-Low expression in kidney and brain			
	FMO5	-Liver			
Cynomolgus macaque	FMO1	-Kidney			Uno et al., 2013
	FMO2	-Lung, kidney, heart, jejunum			
	FMO3	-Liver, kidney, lung, jejunum			
	FMO4	-Kidney, liver, lung, jejunum			
	FMO5	-Liver, lung, jejunum			
	FMO6	-Low expression in all tissue			
Oryctolagus cuniculus	FMO1	-Liver, intestinal mucosa			Larsen-Su et al., 1999; Shehin-Johnson et al., 1995
	FMO2	-Lung	-FMO2 levels in the fetal lung are high at late gestation (except for day 28). After parturition, FMO2 levels fall dramatically,		

		followed by significant recovery by 21 days after birth
FMO3	-Liver (lower expression level than that of FMO3)	
FMO4	-Low expression	
FMO5	-Liver	

183

184 **1.2 From early reports to recent advances in FMO-mediated synthesis**

185 In 1979, the catalytic model of mammalian FMOs was proposed based on spectrum and
186 kinetic studies of pig FMO (pFMO) (Poulsen and Ziegler, 1979). In 1980, the catalytic
187 C4a-(hydro)peroxide intermediate was discovered (Ball and Bruice, 1980), which was
188 further demonstrated in 1981 (Beaty and Ballou, 1981a, 1981b). In 2008, the structure
189 of mFMO was resolved at a 2.6 Å resolution (Fig. 4A) (Alfieri et al., 2008). In 2019, the
190 structural movements of FMOs responding to different classes of substrates were
191 unraveled (Fürst et al., 2019b).

192 The earliest record of indigo biosynthesis arises from the study of naphthalene
193 dioxygenases (Ensley et al., 1983). In 1989, the pBS959 plasmid was constructed based
194 on the naphthalene dioxygenase gene and pUC19 plasmid, which realized the synthesis
195 of indigo in recombinant *E. coli* (Boronin et al., 1989). In 1993, a recombinant *E. coli*
196 capable of producing indigo from glucose was also developed (Murdock et al., 1993).
197 However, the yield was only 135 mg/L. The indigo synthesis pathways of other
198 aromatic hydrocarbon-degrading bacteria were also identified. In 1997, two

199 indigo-synthesizing strains, *Pseudomonas putida* S12 and CA-3, were identified
200 (O'Connor et al., 1997). The toluene dioxygenases from *P. putida* NCIB11767 (Stephens
201 et al., 1989) and *P. putida* F1 (Woo et al., 2000) both demonstrated the ability to
202 synthesize indigo. However, the ability to synthesize indigo of naphthalene
203 dioxygenases and toluene dioxygenase is limited, and their production capacity fails to
204 exceed 300 mg/L. Other classes of oxidases, such as toluene-4-monooxygenase from *P.*
205 *mendocina* and functional enzymes similar to Multicomponent phenol hydroxylases in
206 *Acinetobacter* sp. ST-550 (Doukyu et al., 2002; Doukyu et al., 2003) can also synthesize
207 indigo, but their yield are inferior to mFMO, which has been widely studied for indigo
208 biosynthesis. Choi et al. were the first to report synthesizing indigo by mFMO
209 effectively in 2003 (Choi et al., 2003). Subsequent research on mFMO-catalyzed indigo
210 biosynthesis was based on this study. With further optimization of the sequence and
211 fermentation process (Han et al., 2008), Han et al. reported an indigo yield of 911 mg/L
212 in recombinant *E. coli* (Han et al., 2011). By adjusting cysteine concentration in the
213 tryptophan medium, the production of indigo was increased. In later studies, it was
214 found that cysteine also had a significant impact on the catalytic selectivity of mFMO.
215 During the oxidation catalytic process, the concentration of cysteine increased, and the
216 reaction tended towards the indirubin synthesis (Kim et al., 2019), which is of great
217 significance to the synthesis of indirubin by mFMO. Numerous indigo-producing
218 bacterial FMOs were also reported (Ameria et al., 2015; Lončar et al., 2019a). However,

their yields were not comparable to mFMO. To overcome the limitations of indigo and indirubin biosynthesis by FMOs, various methods were employed, including enzyme engineering and fermentation engineering (Chen et al., 2021; Hsu et al., 2018; Lončar et al., 2019b; Sun et al., 2022).

2. Structures and catalytic mechanisms

2.1 The structure and catalytic mechanism of mammalian FMOs, for instance, AncFMO3-6

The catalytic mechanism of AncFMOs is similar to that of human FMOs, with sequence identities ranging from 82% to 92%. The resolved structures of AncFMOs provide valuable insights into the catalytic mechanism and functions of mammalian FMOs (Nicoll et al., 2020).

Residues 510-532 of AncFMO3 form two α-helices that anchor AncFMO3 tightly to the membrane in a highly hydrophobic transmembrane area (pale green in Fig. 3). AncFMO3-6 also contains two strictly conserved Rossmann fold binding areas for FAD (residues 2–154 and 331– 442, pale cyan in Fig. 3) and NADP(H) (residues 155–213 and 296–330, light blue in Fig. 3). An insertion constructed by three α-helices (orange in Fig. 3), creates a ridged triangular fold that masks the FAD and the catalytic site (Fig. 3B), providing a tunnel from the membrane to the catalytic cavity (Fig. 3C). This structure suggests that substrates enter the blocked catalytic cavity from the tunnel.

Ser62 of AncFMO3-6 can form hydrogen bonds with the N3 atom of the isoalloxazine ring and orientate the FAD towards the catalytic cavity (Fig. 3E). Additionally, Asn61, which is well-conserved in human FMOs near the C4a of the isoalloxazine ring, stabilizes the C4a-(hydro)peroxide intermediate. Mutations of Asn61 cause trimethylaminuria. The residue Leu375 protects the catalytic cavity from solvents.

----------Fig 3----------

2.2 The structure and catalytic mechanism of mFMO

Ongoing studies have described the complete catalytic model of FMOs (Ziegler, 1993) (Fig. 4E). The procedure involves five steps, including (1) FAD reduction to $FADH_2$ by NADPH and an additional H^+, (2) interaction of $FADH_2$ with O_2 to form a stable C4a-(hydro)peroxide intermediate, (3) single oxidation of the closing substrates without particular binding, (4) discharge of the residuary oxygen atom as H_2O, and (5) the whole cycle returns to the initial state when $NADP^+$ is separated from FMO. Since substrates do not need to provide reducing potential and specifically bind to FMO, they are extensive. Theoretically, any nucleophilic compound that could get close to FAD-OOH can become a substrate of FMO. However, molecular size and charges affect the selectivity of FMO. Substrates with one positive charge have the highest affinity to FMO (Ziegler, 2002).

mFMO has 456 amino acids and automatically forms homodimers *in vivo* (Alfieri et al., 2008) (Fig. 4A) and is not a membrane-associated protein like hFMO. There is one Rossmann fold binding area for FAD (1-169 and 281-461, pale cyan in Fig. 4), one Rossmann fold binding area for $NADP^+$ (170–280, light blue in Fig. 4), and three loops (44-80, 166-186, and 276-306, pale green in Fig. 4) linking the above two domains, lacking secondary structural elements. Both FAD and NADPH are the necessary cofactors of FMO. FMO oxidizes substrates by transferring the oxygen atom from C4a. At the same time, NADPH facilitates the reduction of FAD by transferring the hydrogen atom from C4 to N5. Additionally, NADPH's existence is essential for the stability of the C4a-(hydro)peroxide intermediate (Catucci et al., 2020). $NADP^+$ masks the catalytic cavity, providing a proper H-bonding environment that probably protects N5 of the flavine from solvents, maintains the catalytic intermediate, prolongs the intermediate half-life, and offers more chances to react. Tyr212 is a critical amino acid that assists the ribose of $NADP^+$ to protect NADPH from solvent interference (Fig. 4D). Tyr212 and residues 407-415 could facilitate the approach of substrates and catalytic intermediates. Consistent with the findings, our AutoDock (Morris et al., 2009) data indicate that Tyr212 also affects the catalytic process (Fan and Xie, 2023). Specifically, we found that Tyr212 can restrict the size of the catalytic cavity, limit the dimensions of substrates, and protect substrates from solvents, functioning as a "doorkeeper" (Fig. 5B). Moreover, Trp47 is an important residue for the rate of hydride transfer from NADPH to the flavin

279 (Han et al., 2013).

280 The AutoDock simulation revealed that Asn78 is in the catalytic cavity and
281 proximity to indole, FAD, and NADP(H). We believe that Asn78 plays an important role
282 in the catalytic process. Indole was found to be contained in the catalytic cavity, forming
283 hydrogen bonds with NADP(H), and closing the isoalloxazine ring of FAD (Fig. 5A).

284

285 **----------Figs 4, 5----------**

286

287 **Table 2**. The K_{cat} and K_m of different FMO subtypes on various substrates

FMO subtypes	Substrates	$K_{cat}(S^{-1})$	$K_m(\mu M)$	$K_{cat}/K_m(S^{-1}M^{-1})$	References
AsFMO [a]	Allyl mercaptan	0.75 ± 0.01	(1 ± 0.1) × 10^3	(0.75 ± 0.08) × 10^3	Valentino et al., 2020
	L-cysteine	1.7 ± 0.03	(5 ± 0.4) × 10^3	(0.34 ± 0.03) × 10^3	
	N-acetyl L-cysteine	0.57 ± 0.004	(7 ± 0.4) × 10^3	(0.08 ± 0.005) × 10^3	
AncFMO2	Methimazole	0.19 ± 0.01	106 ± 22		Nicoll et al., 2020
	Thioanisole	0.3 ± 0.02	6.9 ± 1.6		
	Trimethylamine	0.16 ± 0.008	445 ± 74		
	NADPH	0.32 ± 0.05	7.8 ± 1.4		
	$NADPH_{uncoupling}$	0.02 ± 0.001	20 ± 5.4		
AncFMO3-6	Methimazole	0.19 ± 0.005	21 ± 2.3		
	Thioanisole	0.1 ± 0.008	128 ± 38		
	Trimethylamine	0.24 ± 0.01	41 ± 6.3		
	NADPH	0.13 ± 0.008	3.5 ± 0.86		
	$NADPH_{uncoupling}$	0.022 ± 0.002	16 ± 5.4		
AncFMO5	Heptan-2-one	0.07 ± 0.003	6.36 ± 1.2		
	NADPH	0.06 ± 0.001	6.48 ± 0.38		
	$NADPH_{uncoupling}$	0.03 ± 0.001	2.1 ± 0.5		
bFMO [a]	Indole	0.22 ± 0.01	(0.98 ± 0.12) ×	(0.22 ± 0.02) × 10^3	Sun et al.,

			10^3		2022
	Indole (K223R/D317S)	0.79 ± 0.03	(0.55 ± 0.14) × 10^3	(1.45 ± 0.30) × 10^3	
MBP-cFMO [a]	Trimethylamine	2.6	575	4521.7	Jung et al., 2018
	Thiourea	0.67	380	1750	Ameria et al., 2015
	Cysteamine	1.83	6000	300	
hFMO1 [a]	Methimazole	1.07	7		Furnes and Schlenk, 2004
	Imipramine	0.85	14		
	Fenthion	1.55	340		
	Methyl p-tolyl sulfide	0.767	284		
hFMO2	Thiourea	0.85	27		Henderson et al., 2004
	Phorate	0.683	57		
	Ethylene thiourea	0.833	14		Krueger et al., 2002b
	a-Naphthylthiourea	0.55	42		
	1-Phenylthiourea	0.4	29		
	Disulfoton	0.333	32		Krueger et al., 2002a
hFMO3	Benzydamine	3.12 ± 0.20 (min^{-1})	52.0 ± 9.0		Bortolussi et al., 2021
	Tamoxifen	1.13 ± 0.70 (min^{-1})	6.40 ± 0.70		
	Fenthion	0.183	145		Furnes and Schlenk, 2004
	5-DPT	0.85	155		Cashman et al., 2000
	Trimethylamine	3.15	32		
	Tyramine	1.833	231		
Truncated hFMO3	Benzydamine	4.51 ± 0.18 (min^{-1})	53.0 ± 6.1		Bortolussi et al., 2021
	Tamoxifen	1.63 ± 0.01 (min^{-1})	5.60 ± 0.30		
mFMO [a]	Trimethylamine	7.3 ± 0.6	6.1 ± 0.1	(8.4 ± 0.7) × 10^5	
	Trimethylamine (E158A/E159A)	7.1 ± 1	6.4 ± 0.3	(9.0 ± 1) × 10^5	
	Nicotine	130 ± 30	3.0 ± 0.2	(2.3 ± 0.6) × 10^4	Alfieri et al., 2008
	Methimazole	66 ± 7	1.0 ± 0.02	(1.5 ± 0.2) × 10^4	
	N, *N* dimethylaniline	232 ± 28	1.8 ± 0.4	(7.8 ± 2) × 10^3	
	Indole	90 ± 14	0.7 ± 0.03	(7.8 ± 1) × 10^3	

	Trimethylamine	23 (nmol/min/mg protein)	19		
	Cysteamine	29 (nmol/min/mg protein)	180		Choi et al., 2003
	Thiourea	17 (nmol/min/mg protein)	390		
NiFMO [a]	Trimethylamine	2.01 ± 0.08	45.6 ± 9.6	44,000	
	Methimazole	1.10 ± 0.08	77 ± 10	14,000	
	Pyrrole	0.69 ± 0.03	46 ± 17	4,800	
	Indoline	0.70 ± 0.03	98 ± 14	7,100	Lončar et al., 2019a
	Indole	0.11 ± 0.01	137 ± 23	730	
	6-Bromoindole	0.09 ± 0.03	640 ± 340	140	
	Tris(hydroxymethyl) aminomethane (TRIS)	0.18 ± 0.02	21500 ± 5600	9	
pFMO1 [a]	Dihydrolipoic acid		1700		Taylor and Ziegler, 1987
	Lipoic acid		120		
	Trimethylamine		617		Sabourin and Hodgson, 1984
rFMO2 [a]	n-Heptylamine		27,000		
	N-octylamine		6700		
	N-nonylamine		1800		Tynes et al., 1986
	N-decylamine		400		
	N-undecylamine		90		
	N-dodecylamine		33		
	N-tridecylamine		13		

[a] As = *A. sativum*; b = *Methylophaga aminisulfidivorans*; c = *Corynebacterium glutamicum*; h = *Homo sapiens*; m = *Methylophaga sp.* strain SK1; Ni = *Nitrincola lacisaponensis*; p = *Sus scrofa*; r = *Oryctolagus cuniculus*.

3. The application of FMO in biosynthesis

3.1 The advantages of FMO among enzymes in indigo biosynthesis

In the field of indigo biosynthesis, researchers aim to achieve higher bio-yield and simpler production conditions. FMO is currently the most studied enzyme in this regard and is particularly prominent in these two aspects. While there are reports on the biosynthesis of indigo using other enzymes, most of them remain at the primary level of "observed phenomena".

For instance, Cytochrome P450 monooxygenases have been observed to synthesize indigo under specific conditions (Fiorentini et al., 2018; Kim et al., 2018), but their biosynthetic ability has not been thoroughly explored, perhaps due to the characteristics and productive ability of the enzyme. Similarly, multicomponent enzymes without heme, such as Naphthalene dioxygenases (Doukyu et al., 2002; Pathak and Madamwar, 2010; Groeneveld et al., 2016) and multicomponent phenol hydroxylases (Doukyu et al., 2003; Qu et al., 2012a), have been used as biocatalysts, but their application is limited by the fermentation conditions. The yield of indigo synthesized by these enzymes has not exceeded 300mg/L due to the need for stable conditions for each component, which makes FMOs with simple components more practical for utilization.

Furthermore, it has been shown that D flavoprotein monooxygenases, a close relative of FMO, can synthesize indigo (Dai et al., 2019), but further research is needed to understand the underlying mechanism on the biosynthetic level.

3.2 FMO-Catalyzed Biosynthesis of Indigo

FMOs possess a unique oxidative catalytic mechanism, and their application in biosynthesis, particularly in the synthesis of indigoid compounds, has been extensively studied (Table 3). Indigo, one of the oldest textile dyes, has traditionally been produced through plant extraction or chemical synthesis (Stasiak et al., 2014). However, to develop an environmentally friendly strategy, biosynthesis of indigo using microorganisms has been proposed (Qu et al., 2010; Honda et al., 2008; Qu et al., 2012b), and engineered *E. coli* has been validated for indigo biosynthesis (Ensley et al., 1983; Murdock et al., 1993; Berry et al., 2002; Doukyu et al., 2003). The discovery of mFMO from *Methylophaga* sp. strain SK1 has significantly improved the efficiency of heterologous biosynthesis of indigo (Choi et al., 2003).

In the biosynthetic strategy, indole is used as a substrate or intermediate in the pathway. With the help of heterologous FMO, indole is oxidized to 3-hydroxyindole (indophenol/hydroxyindole), which further forms indigo by spontaneous dimerization under aerobic conditions (Choi, 2020; Han et al., 2008). However, the productivity of the original plasmid carrying mFMO was limited, and optimization of the engineered plasmid was implemented. After removing the redundant sequences, the indigo yield of the improved plasmid reached 662 mg/L, an increase of 413% compared to the initial production of 160 mg/L (Han et al., 2008). Moreover, a yield of 920 mg/L in a 5L fermenter was achieved, and a larger scale fermentation system was developed, which

achieved a yield of 911 ± 22 mg/L of indigo in a 3,000 L fermenter with an input of 2 g/L of tryptophan (Han et al., 2011).

Numerous studies have been conducted to improve the properties of the enzyme and optimize biosynthetic conditions (Table 3). For instance, a consecutive two-cell reaction system was constructed using mFMO, 6-halogenase SttH, and tryptophanase TnaA to synthesize 6,6'-dibromoindigo (6BrIG) with a yield of 315.0 mg/L from tryptophan (Lee et al., 2021). The redox reaction of FAD cofactor, which tightly links with FMO, depends on the assistance of NADPH (Alfieri et al., 2008; Krueger and Williams, 2005). To recycle NADPH, an optimized strategy of fusing mFMO and phosphate dehydrogenase (PTDH) was proposed to utilize phosphate as a cheap and sacrificial substrate (Rioz-Martinez et al., 2011). This bifunctional enzyme, mFMO-PTDH, not only exhibits the ability to oxidize indole and its analogs but also shows potential for chirality selection in the biocatalytic sulfoxide oxidation of prochiral sulfides (Pereira et al., 2022; Schnepel et al., 2021; Wojaczyńska and Wojaczyński, 2020). Moreover, directed evolution was applied for mFMO modification, and some mutants exhibited higher K_{cat} and lower K_m, showing higher indole affinity and superior catalytic efficiency at low substrate concentrations (Lončar et al., 2019b).

Since indigo itself is insoluble in water, it requires the addition of reductants such as sodium sulfate to modify it into a water-soluble dye in practical production, which increases economic and environmental burdens. A novel strategy of chemical group

353 protection was proposed to effectively solve the insolubility problem of indigo in water.
354 A glycosyltransferase from *Polygonum tinctorium* was co-expressed with mFMO in *E.*
355 *coli* to introduce a glucose group to protect the active hydroxyl group of hydroxyindole
356 and form a water-soluble and stable indican to prevent indigo from further oxidation
357 (Hsu et al., 2018). Subsequently, by adding glucosylase to remove the protective groups,
358 the production of indigo was restored, showing excellent practical properties. To reduce
359 the substrate cost of indigo fermentation, a system based on the co-cultivation of
360 microorganisms was developed to convert renewable carbon substrates to indigo (Chen
361 et al., 2021). The system can be divided into upstream and downstream parts: the
362 upstream engineered *E. coli* is responsible for the synthesis of tryptophan from glucose
363 or glycerol; the downstream system is responsible for the conversion of tryptophan to
364 indole and then to indigo. Besides, the metabolism of the two strains was specially
365 optimized, and the final indigo yield reached 104.3 mg/L, which was more than eleven
366 folds higher than the original strain.

367 Recently, a strategy was implemented to increase the cyclopropane fatty acid (CFA)
368 composition of phospholipid fatty acids in the cell membrane to counteract the
369 cytotoxic effects of indole. This approach resulted in a 1.5-fold increase in indigo
370 production compared to the control strain (Ham et al., 2023). Additionally, the enzyme
371 TRP can convert tryptophan into indole and pyruvate (Shimada et al., 2004). As
372 pyruvate can be used by the cell to regenerate NADPH, a bifunctional fusion enzyme of

373 mFMO-TRP was developed to produce indigo from L-tryptophan. This approach
374 resulted in the complete conversion of 2.0 g tryptophan into 1.7 g indigo per liter of
375 culture (Fabara and Fraaije, 2020).

376 In addition to mFMO, other FMOs isolated from various organisms have shown
377 potential for synthesizing indigo compounds. For instance, FMO motifs encoded by
378 *Mesorhizobia* and *Sphingomonas* isolated from wastewater sludge by metagenomic
379 methods exhibit biocatalytic activity for indigo synthesis (Singh et al., 2010). PtFMO
380 was cloned from *P. tinctorium* and heterologously expressed in *E. coli* BL21 (DE3),
381 achieving a 30 mg/L indigo yield (Inoue et al., 2021). The cFMO, cloned from
382 *Corynebacterium glutamicum*, reaches the biosynthetic indigo yield of 685 mg/L
383 (Ameria et al., 2015) in engineered *E. coli*. Mutants F170Y, A210G, A210S, and T326S
384 cFMOs were fused with maltose-binding protein (MBP), and the fusion protein
385 produced 1,040 mg/L indigo and 112 mg/L indirubin with 2.5 g/L tryptophan (Jung et
386 al., 2018). While NiFMO from *Nitrincola lacisaponensis* has a comparably lower yield
387 of indigo, it exhibits unique thermal stability, and the optimum catalytic temperature
388 reaches 51 ℃, which is about 8 ℃ higher than mFMO (Lončar et al., 2019a).

389 In summary, the biosynthesis of indigo using microorganisms has been proposed as
390 an environmentally friendly strategy, and the discovery of mFMO has significantly
391 improved the efficiency of heterologous biosynthesis of indigo. Various studies have
392 been carried out to optimize the biosynthetic conditions and improve the properties of

the enzyme, which contributes to the development of efficient strategies for indigo production. A discussion of potential strategies to improve yields is included in the 3.4 subsection.

3.3 FMO-Catalyzed Biosynthesis of Indirubin

Utilizing the improved mFMO (Han et al., 2008), the biosynthetic pathway of indirubin was further studied. Cysteine was found to increase the selectivity of FMO for 2-hydroxyindole (Han et al., 2012), leading to a yield of 223.6 mg/L under optimum conditions. In 2022, a semi-rational design was applied and combined modification to the two regions (K223R/D317S) of FMO. Based on metabolic engineering technology, *E. coli* strains were screened to obtain high indirubin production, reaching the current maximum yield of 860.7 mg/L (Sun et al., 2022).

To reduce substrate costs in fermentation, researchers have employed mFMO and *E. coli* tryptophanase (TRP) to facilitate the biological synthesis of indirubin utilizing glucose as the primary substrate. As a result, a notable yield of 0.056 g/L of indirubin has been accomplished (Du et al., 2018).

Table 3. The summary of production of indigo/indirubin by FMOs

Year	Strategies	Genetic sources of FMO	Chassis	Plasmid/ Promoter	Production of indigo/indirubin (mg/L)	Supplements in culture	References
2003	First clone mFMO	*Methylophaga sp.* SK1	*E. coli* DH5α	pBlue 2.0	indigo: 160	2.00 g/L tryptophan	Choi et al., 2003
2008	Gene sequence	*Methylophaga*	*E. coli*	pBlue 1.7	indigo: 920	2.40 g/L	Han et al.,

	and culture optimization	*aminisulfidivorans* MPT	DH5*α*			tryptophan	2008
2011	Batch and continuous fermentation	*Methylophaga aminisulfidivorans* MPT	*E. coli* DH5*α*	pBlue 1.7	indigo: 911 ± 22	2.00 g/L tryptophan	Han et al., 2011
2012	Cysteine influences the regioselectivity	*Methylophaga aminisulfidivorans* MPT	*E. coli* DH5α	pBlue 1.7	indirubin: 223.6	2.00 g/L tryptophan, 0.36 g/L cysteine	Han et al., 2012
2015	First clone cFMO	*Corynebacterium glutamicum*	*E. coli* WCO21	pMCF14	indigo: 685 indirubin: 103	2.50 g/L tryptophan	Ameria et al., 2015
2018	Site-directed mutagenesis	*Corynebacterium*	*E. coli* WTS326	pK-T326S	indigo: 1,040 indirubin: 112	2.50 g/L tryptophan	Jung et al., 2018
2018	Biochemical protecting group for dyeing	*Methylophaga aminisulfidivorans*	*E. coli* MG1655	pTMH561	indigo: 400	3.10 g/L tryptophan	Hsu et al., 2018
2020	Plant origin	*Polygonum tinctorium*	*E. coli* BL21	pET19b	indigo: 30	0.80 mM tryptophan	Inoue et al., 2021
2020	Fusion expression	*Methylophaga sp.* SK1	*E. coli* NEB10β	pBAD	indigo: 1700	2.00 g/L tryptophan	Fabara and Fraaije, 2020
2021	Co-culture	*Methylophaga aminisulfidivorans* MPT	*E. coli*	pCDFDuet-1	indigo: 104.3	5.00 g/L glucose or glycerol	Chen et al., 2021
2022	Structure-guided enzyme engineering	*Methylophaga aminisulfidivorans* MPT	*E. coli* BL21	pET28a	indirubin: 860.7	2.00 g/L tryptophan, 0.36 g/L cysteine	Sun et al., 2022
2023	Regulate the permeability of the cell membrane	*Methylophaga aminisulfidivorans*	*E. coli* BL21	pCDFDuet-1	indigo: 1080	10.00 mM tryptophan	Ham et al., 2023
2023	Producing isobutanol and indigo together	*Methylophaga aminisulfidivorans*	*E. coli* BL21	pETDeut-1	isobutanol: 5800 indigo: 194.1	5.00 mM tryptophan	Cho et al., 2023

410

3.4 Strategies for improving FMO-catalyzed biosynthesis

In 2023, silkworms were used to synthesize indigo, which opens a new avenue (Jia et al., 2023). Although researchers have achieved a yield of 1700 mg/L of indigo (Fabara and Fraaije, 2020), depending on tryptophan as the substrate and the lack of industrialization of indigo biosynthesis indicate the need of further improvements if we plan to use biotechnology as a substitute for the chemical method. Remodeling of FMOs, such as directed evolution and *de novo* design, holds promise for achieving higher yields. Additionally, few researchers have studied indigo biosynthesis using eukaryotes like yeasts as the chassis (Fig. 9A). To increase the yield of indigo synthesized by FMOs, several approaches can be pursued.

3.4.1 Insights from FPMOs

To explore the potential of FMOs in indigo production, one effective approach is to examine studies on other enzyme families with similar mechanisms, such as flavoprotein monooxygenases (FPMOs).

Within the FPMO class B, which uses NADPH as a coenzyme, there are three subgroups, including FMOs, microbial N-hydroxylating monooxygenases (NMOs), and Baeyer-Villiger monooxygenases (BVMOs) (Paul et al., 2021; van Berkel et al., 2006). BVMOs can produce 0.031 g/L indirubin with 1 mM indole and 5 mM cysteine and convert indole to indigo only after specific mutations (Pazmiño et al., 2007; Catucci et

al., 2022). A mutant BVMO from *Acinetobacter radioresistens* (ArBVMO) with the R292A mutation can efficiently produce indigoids, with a k_{cat} of 0.12 s^{-1} for indigo production. It can synthesize 0.138 g/L indirubin from 5 mM indole and 5 mM cysteine, slightly lower than that of mFMO (Catucci et al., 2022). As cysteine enhances the selectivity of FMOs for indirubin production, ArBVMO is regulated in the same way, indicating that their structure of regulation is similar.

Styrene monooxygenase (SMO), which belongs to the FPMO class E, can convert tryptophan to indigo (Cheng et al., 2016; Pan et al., 2023). The maximum yield of indigo produced by SMO was up to 787.25 mg/L after 24 hours of fermentation with 2.0 g/L tryptophan as substrates (Pan et al., 2023). Further research on indigo production by different FPMOs is recommended, as the functional conservation between these enzymes offers potential for the *de novo* design in the future.

While there is little research on the random mutagenesis of FMOs, researchers have successfully redesigned several other monooxygenases, including SMOs (Tan et al., 2019) and cyclohexanone monooxygenases (CHMOs) (Zhang et al., 2019), resulting in significantly increased catalytic activity. For example, CHMO, a BVMO named for their natural substrate cyclohexanone, was performed both local and global protein engineering using two Casting libraries surrounding FAD^+ and $NADP^+$ prosthetic groups, as well as an error-prone PCR library of the full-length CHMO. This resulted in a 50-fold increase in activity compared to the previously best-performing variant

(Zhang et al., 2019). As the structure of mFMO resembles BVMOs in their coenzyme binding mode (Alfieri et al., 2008; Paul et al., 2021), it is possible that random mutagenesis could enhance the catalytic activity of mFMO and increase indigo production.

3.4.2 Directed evolution

Although FMOs (EC 1.14.13.8) are of high interest in biotechnology due to their ability to catalyze various regioselectivity and stereoselectivity monooxygenation reactions (Catucci et al., 2017; Mitsubayashi and Hashimoto, 2000), natural enzymes have inherent limitations that restrict their industrial utilization in indigo production (Ameria et al., 2015; Choi, 2020; Ma et al., 2018; Rioz-Martinez et al., 2011). Therefore, in recent years, there has been an increasing number of publications focusing on enzyme engineering to improve enzymes' catalytic activity, specificity, regioselectivity, stereoselectivity, thermostability and solvent tolerance (Choi, 2020; Fabara et al, 2020; Linke et al., 2023).

Over the past two decades, many enzyme engineering strategies have been developed, with directed evolution being the most studied (Fig. 6) (Chowdhury and Maranas, 2020; Qi et al., 2022; Xiong et al., 2021). The concept of directed evolution is a natural evolution process through iterative cycles of genetic diversification followed by high-throughput screening or selection (Xiong et al., 2021). This concept emerged

early in 20th century and continued to develop in the 1990s. Three types of methods were identified for randomly generating mutants and *in vitro* recombination (Xiong et al., 2021). The first type is error-prone PCR, based on oligonucleotide mutagenesis (Cadwell and Joyce, 1992), which was first described in 1989 (Lenug D, 1989). The second type of methods is based on homologous recombination, including DNA shuffling (Kikuchi et al., 2000), staggered extension process (StEP) (Zhao et al., 1998), random priming *in vitro* recombination (RPR) (Shao et al., 1998), and random chimeragenesis on transient templates (RACHITT) (Coco, 2003). Finally, the third type of methods includes incremental truncation for the creation of hybrid enzymes (ITCHY) (Hu et al., 1997), random multi-recombinant PCR (RM-PCR) (Tsuji et al., 2001), and sequence homology-independent protein recombination (SHIPREC) (Sieber et al., 2001).

----------**Fig 6**----------

In 2003, a mutant generation and clone screening approach was utilized with a flow cell optical rotation and a UV detector to engineer FMOs from *Oryctolagus cuniculus* (rFMO) and *Rhesus macaque* (rmFMO) for stereochemical preference control in the sulfoxidation of methyl p-tolyl sulfide. The engineered rFMO displayed up to 35% increased activity (Polyzos, 2003), meeting the demand. Furthermore, unspecific

peroxygenase (UPO, EC 1.11.2.1), a type of heme-thiolate enzyme with self-sufficient monooxygenase activity, can also catalyze the reaction from indole to indigo. The *Agrocybe aegerita* UPO1-encoding gene was subjected to directed evolution in *Saccharomyces cerevisiae*, and after five generations of evolution, nine mutations were screened, resulting in a 3250-fold activity improvement with no alteration in protein stability (Molina-Espeja et al., 2014). Additionally, after directed evolution, the half-life of a peroxidase (EC 1.11.1.16) increased from 3 to 35 minutes in the presence of 3000 equivalents of H_2O_2 and with a 6 °C upward shift in thermostability (Gonzalez-Perez et al., 2014).

3.4.3 Semi-rational design of FMOs

Referring to enzyme engineering reviews (Xiong et al., 2021), semi-rational design strategy generates a mutation library on specific amino acid residues based on sequence and structural information of enzyme protein. This strategy avoids the time-consuming and labor-consuming process in directed evolution and has a convenient screening of suitable results. Semi-rational design strategy is based on two methodologies. In the sequence-based enzyme redesign method, critical conserved residues binding to substrate are identified through multiple sequence analysis of homologous protein sequences (Fig 5). In contrast, in the structure-based enzyme redesign method, the functional hot spots are pinpointed by analyzing substrate, transition state, or product

binding in the active site using docking results (Fig 4). Eventually, site-directed mutation and site-directed saturation mutation libraries are constructed and then screened for new functional enzymes.

To date, using site-directed mutagenesis, several studies have identified the role of amino acid residues associated with the structure and function of FMOs, accumulating a wealth of information on residue-function association (Wyatt et al., 1998). This information provides a valuable source for enzyme semi-rational design. For example, hFMO3 was researched through semi-rational design in different aspects. Numerous hFMO3 allelic variants were identified in patients and the 3D structural model of hFMO3 was generated by homology modeling, which was soon used to perform molecular dynamics simulations, followed by structural mapping of 12 critical polymorphic variants and molecular docking experiments with five different known substrates of hFMO3, giving insights into their binding mechanism (Gao et al., 2016).

A computational library design protocol named FRESCO is an structure-based enzyme engineering tool for stabilization (Wijma et al., 2018). In 2019, this protocol was first performed on cyclohexanone monooxygenase (EC 1.14.13.22), resulting in 128 screened point mutants. The most stable and highly active mutant displayed an increase in unfolding temperature of 13 °C and an approximately 33-fold increase in half-life at 30 °C (Fürst et al., 2019a). Then, after discovering the thermostable NiFMO (Lončar et al., 2019a), FRESCO was utilized to improve its thermostability. After

screening a relatively small number of enzyme mutants, the k_{cat} for indole was improved by 1.5-fold (Lončar et al., 2019b). Furthermore, in 2022, the catalytic efficiency of bFMO, cloned from *Methylophaga aminisulfidivorans*, was enhanced by 6.6-fold using FRESCO (Sun et al., 2022). Moreover, a recent study engineered mFMO for industrial application using the Protein Repair One-Stop Shop (PROSS) algorithm (Goldenzweig et al., 2016; Peleg et al., 2021; Wijma et al., 2018) and successfully redesigned a mutant with the ability to reduce TMA levels in a salmon protein hydrolysate at industrially relevant temperatures (Goris et al., 2023).

Further improvements could be made to FMOs in their industrial utilization for producing indigo. In 2016, a study combining structural analysis and sequence alignment successfully switched the cofactor preference of type I BVMOs from NADPH to NADH (Beier et al., 2016). As NADH cofactor is preferred for industrial purposes, this redesign could be a promising future project to apply to FMOs to acquire better industrial properties.

3.4.4 *De novo* enzyme design with high substrate specificity

Recently, the limitations of directed evolution or semi-rational design strategies have become apparent due to their mutation rates, making it difficult to satisfy stability or specific activity needs for certain applications. *De novo* protein design is an emerging method for enzyme engineering that can generate a sequence based on the given

structure (Chen et al., 2022; Wang et al., 2023; Xiong et al., 2021). Computational physics-based tools for *de novo* design, such as dynamics simulation and optimizing sequences based on a given structure (Ferreira et al., 2022), can highly assemble naturally existing enzymes. Additionally, AI tools for protein design, which can generate *de novo* motifs or "hallucinate" a compatible structure based on the input structure backbone (Anishchenko et al., 2021), have become a new trend in life science (Ding et al., 2022; Kim et al., 2021; Liu and Chen, 2022; Yang et al., 2023). It is worthwhile to describe some of the most exciting tools that have been developed in recent years and their powerful potential applications in the industrialization of FMOs.

De novo design strategies have rapidly developed through energy computing and the development of protein modeling (Wang et al., 2023; Woolfson, 2021). There are two types of protein modeling mechanisms, which are correlated to different tools. The first type is the template-based protein modeling, which is based on multiple sequence alignment (MSA) and residue-residue interaction (RRI) data. Some successful AI-based programs in this category include AlphaFold-2, RoseTTAFold, and I-TASSER. The second type is non-template-based protein modeling, which used methods of Monte Carlo (MC) or Markov Chain Monte Carlo (MCMC) simulations to get the protein to fold into its energy-minimized state.

Introductions for bioinformatics tools developed for *de novo* enzyme design are shown in Table 4, such as RoseTTAFold (Wang et al., 2022), Message-Passing Neural

571 Network (MPNN) (Dauparas et al., 2022), RFdiffusion (Watson et al., 2023), and
572 Family-wide hallucination (Yeh et al., 2023). Each tool has its own advantages and
573 limitations.
574
575 **Table 4**. The summary of various *de novo* design tools

Protein design tools	Input	Function	Advantages	Shortcomings	Remarks	References
1. Protein structure prediction						
AlphaFold2	Protein sequences (MSA)	Deep learning-based protein structure prediction	High accuracy	1. High computational resource requirements; 2. Limited accuracy; 3. Cannot predict novel structures	As a baseline model for protein structure prediction, the model is modified for protein design.	Jumper et al., 2021
RoseTTAFold	Protein sequences	Deep learning-based protein structure prediction		1. Limited to specific issues; 2. Energy function limits	Introduce energy function to consider the rationality of protein structure, variant tools based on specific tasks can be flexibly applied to protein design	Wang et al., 2022
trRosettaX2	Protein sequences (MSA)	Deep learning-based protein structure prediction	More accurate than AlphaFold2	Multimer structure prediction	Monomer and Multimer structure predictions were ranked at the top and fourth in CASP15	Peng et al., 2023
ESMFold	Protein sequences	Deep learning-based protein	1. Protein-specific prediction; 2. Faster than MSA-based solutions	Less accurate than AlphaFold2	A model based on information extracted from	Weissenow et al., 2022

		structure prediction			protein language models might be better for protein design than those based on MSAs	
D-I-TASSER	Protein sequences (MSA)	Template-based protein structure prediction		Not satisfied with multi-domain protein modeling	A model based on the threading method. The server can perform both template-based and template-free modeling	Zheng et al., 2021
2. Physics-based protein design						
TopoBuilder	Ideal secondary structure elements (SSEs) and epitope	Backbone generation	Can construct and design any protein form description	Limits to the guidance of natively arranged SSEs	A fragment-based method works as an extension of the Fold Form Loops protocol	Harteveld et al., 2022
SEWING	Coordinates, sequences, and connectivity information for a set of substructures from native protein	Backbone generation	1. Rapidly generate large numbers of scaffolds; 2. Advantageous for functional design.		Perform structural extension with native-substructure graphs	Guffy et al., 2018
AbDesign	Protein structures of selected protein family	Backbone generation	Large-scale assembly		*De novo* backbone design by assembling local structures	Lipsh-Sokolik et al., 2021
HBNet	Backbone structure	Protein design	Hydrogen-bond networks design		A method that calculates cooperative hydrogen bonding networks should	Boyken et al., 2016

				be broadly useful in enzyme design	
Meta-multistate design	Backbone structure	Sequence optimization	1. Sequence design considering conformationally dynamic state; 2. Large ensemble size	A multistate design method could be used to design multisubstrate enzymes	Davey et al., 2017
Rosetta		Protein modeling and design	1. Many completely Rosetta-based protocols exist; 2. Various web servers	A powerful suite of programs for *de novo* protein design	Leman et al., 2020
IPRO		Protein design	Integrate many computational protein engineering methods	Perform different functions with different modules	Pantazes et al., 2015
OSPREY	Protein structure	Protein modeling and design	With various functions related to protein design based on GPU acceleration	Use a physics-based energy function that combines both Amber and CHARMM	Hallen et al., 2018
ISAMBARD	Natural protein structures or backbones depend on the approaches	Energy prediction	User friendly	A suite of *de novo* biomolecular design tools using BUFF energy function	Wood et al., 2017
Tinker	Protein structure	Molecular mechanics (MM) and molecular dynamics (MD) simulations	1. User friendly; 2. Interoperable with other tools and access to many force fields	The main characteristic of this package is its modularity and has developed a few branches like Tinker-HP and Tinker-OpenMM	Rackers et al., 2018
OpenMM	Support for multiple input pipelines	Protein dynamics simulation	High extensibility	Based on extensibility in every layer of	Eastman et al., 2017

					the architecture, users can easily add new features like novel functional formed forces or new simulation protocols	
GROMACS	Protein structure	Protein dynamics simulation	1. Fast; 2. Various simulations; 3. Able to scale the largest machines in the world		Support simulations including leap-frog Verlet, velocity Verlet, Brownian, and stochastic dynamics, as well as calculations that do energy minimization, normal-mode analysis, and simulated annealing	Abraham et al., 2015
YASARA		Homology modeling, energy minimization, docking, and molecular dynamic simulations	User-friendly with a built-in graphical interface		Can be used as a molecular dynamics refinement for Rosetta to broaden the substrate scope	Land and Humble, 2018
MODIP	Protein sequence	Disulfide bond design	Depends on database		Used in the DSDBASE2.0 database on native and modeled disulfides to identify pairs of residues that form disulfide	Kalmankar et al., 2022

					bonds	
PROPKA	Protein structure	protonation states prediction			A model focuses on the prediction of ligand pK_a values	Søndergaard et al., 2011
MaSIF	Database of known protein structure and protein binding surface information	Protein interaction analysis	The target protein can be searched directly across the mechanism of protein-protein interaction.	1. The conformation of the designed protein is inflexible; 2. The antimutagenicity is not considered; 3. It depends on the binding surface seed bank; 4. The functional goal is single and needs artificial screening and optimization.	Techniques from the field of geometric deep learning are introduced to resolve information encoding protein interaction interfaces	Gainza et al., 2023
3. Statistics-based de novo design						
ProteinMPNN	Coordinates of protein (polymer)	Protein design	1. short calculation time; 2. Able to design new proteins with few restrictions	1. Computational requirements; 2. Hardware memory limitations	For the design of monomeric protein design, the Monte Carlo optimization algorithm and the hallucination strategy are combined, and the loss function is used to ensure the consistent stability of protein folding and assembly.	Dauparas et al., 2022
PoPMuSiC	Protein structure	Energy prediction	1. Rapid computation of stability changes induced by single-site mutation; 2. Good prediction performance; 3. User friendly		Use the statistical energy functions extracted from empirical data	Dehouck et al., 2011
Autodock	Protein structure	Docking	Molecular interactions		A suite of toolkits for	Goodsell et al., 2021

	(with ligand)			various computational ligand docking that has developed over 30 years	
Surflex-Dock	Protein structure (with ligand)	Docking	Superior in predicting the binding mode and binding score	Use a surface-based molecular similarity search engine to rapidly generate a suitable conformation and alignment	Jain, 2003
CSR-SALAD	Protein structure	Cofactor specific switch analysis	User friendly	Perform the switch between NAD and NADP cofactors	Cahn et al., 2018
ABACUS	Backbone structure	Energy prediction	No boundary of homology between design targets and training proteins	Combine a statistical energy function with van der Waals energy terms to search stable sequences for a given backbone structure	Xiong et al., 2017
DenseCPD	Structure (atom distribution information)	Deep learning-based protein sequence design	Quick and convenient to generate *de novo* sequence	Find the most suitable sequences for the protein backbone	Qi and Zhang, 2020
RFdiffusion	Protein structure coordinates with Gaussian noise	Deep learning-based protein design	1. Better generation of diversity; 2. Potential to solve complex problems	The extension of the RoseTTAFold variant tool in the generative diffusion model	Watson et al., 2023

ProtGPT2	Protein sequence	Deep learning-based protein design	Discover new proteins	1. Computational requirements; 2. Hardware memory limitations	Application of GPT2 deep language model	Ferruz et al., 2022
ProteinSGM	Image-like representations of protein structures	Deep learning-based protein design		1. Computational requirements; 2. Cannot analyze inter-chain interactions	Applications of diffusion models and the continuous-time SDE framework	Lee et al., 2023

RoseTTAFold, developed by David Baker laboratory, is a protein structure prediction tool that can be used for designing proteins with specific functions. It is based on two schemes (Fig. 7) (Wang et al., 2022): (1) constrained hallucination (trRosetta or RoseTTAFold) to optimize known functional protein sequence and (2) inpainting (RF_{joint}) to optimize and fill the gaps between two sequences to ensure a reasonable final synthesized protein structure.

Unlike energy optimization-based structure prediction tools such as RoseTTAFold and AlphaFold 2, MPNN (Dauparas et al., 2022) predicts and generates candidate protein sequences for the basic protein skeleton. This tool is useful for oligomers and protein-protein binding application, as it can ensure the formation of binding forms between protein skeletons without blindly pursuing the goal of the lowest energy.

Researchers have developed RFdiffusion (Watson et al., 2023), a new protein

design diffusion model that combines protein structure prediction methods with an in-depth understanding of protein structure. By using Fine-tuning RoseTTAFold as a denoising network in Denoising Diffusion Probabilistic Models (DDPMs), RFdiffusion can generate a variety of design protein skeletons. Through a multi-step denoising process, a design protein skeleton is gradually produced. The MPNN is then used to generate the protein sequence with the desired structure.

----------Fig 7----------

A deep-learning-based 'family-wide hallucination' approach was used to design artificial luciferases with a much higher substrate specificity than native luciferases (Yeh et al., 2023). Based on the successful examples of *de novo* design (Wicky et al., 2022), it is possible to design a new thermostable enzyme that can specifically catalyze indole and form homomultimers. One approach could be using deep network hallucination to generate a wide range of symmetric protein homo-oligomers, specifying the basic number of symmetric units and the length of the oligomer. Then, structure prediction and MPNN could be used to optimize the protein sequence to obtain a "convergent" protein sequence. One approach is Molecular Surface Interaction Fingerprinting (MaSIF) (Gainza et al., 2023), which could be used to predict the protein binding site and encode the protein binding interface to obtain the fingerprint

609 information of the binding interface. With the help of the binding interface fingerprint,
610 the seeds of complementary binding motifs could be generated in the database, and the
611 obtained seeds could be further optimized to obtain the designed protein structure. One
612 approach could start from the natural sequence, carry out Monte Carlo search in the
613 sequence space, and apply trRosetta structure prediction neural network to score the
614 confidence of the predicted structure. By combining these methods, it may be possible
615 to design a new enzyme that meets the desired specifications.
616
617 **3.4.5 The immobilization of FMOs**
618 To meet the economic requirements for enzyme usage, researchers have explored the
619 utilization of immobilized FMOs (Fig. 8). This has been achieved by immobilizing
620 FMOs on silica nanospheres (Biradar et al., 2010) or magnetic nanoparticles (Ramana et
621 al., 2017). Immobilizing at the C-terminal (membrane anchor region) of hFMO3 has
622 been shown to significantly improve its enzymatic thermostability (Gao and Zheng,
623 2019).
624 FMOs on electrodes have been studied, immobilized through dialysis or entrapment
625 in a gel cross-linked with bovine serum albumin and glutaraldehyde (Castrignanò et al.,
626 2010). These immobilized FMO electrodes have been used as biosensors for detecting
627 drug and microelements in electrochemistry (Mitsubayashi and Hashimoto, 2000;
628 Mitsubayashi and Hashimoto, 2002; Saito et al., 2008). Different methods of

immobilization have been studied, and immobilization on the gold surface has been found to be more effective in catalysis (Ferrero et al., 2008; Sadeghi et al., 2011; Sadeghi et al., 2010). The electrochemical response of the GC/DDAB/hFMO3 electrode was enhanced using graphene oxide (Castrignanò et al., 2015; Sadeghi et al., 2010).

----------Fig 8----------

3.4.6 Regenerating NADPH in FMO catalysis

In the catalytic cycle of FMOs, the flavin cofactor is reduced by NADPH to initiate subsequent reactions (Eswaramoorthy et al., 2006). However, in extracellular enzyme reaction systems or recombinant cells, the rate of NADPH regeneration may limit the overall reaction rate. By fusing dehydrogenase with FMOs or constructing recombinants to express these enzymes, researchers have utilized different dehydrogenases for NADPH recycling to overcome this limitation (Doukyu et al., 2003; Rioz-Martinez et al., 2011). The choice of dehydrogenase is based on the substrates catalyzed to refill NADPH, such as phosphite, ethanol, and malate (Pan et al., 2023). The usual function of the FMOs-dehydrogenase dimers for NADPH-regeneration is to supply NADPH or NADH in a catalytic environment that lacks them, such as in organic solvents (Doukyu et al., 2003), where there are abundant organic substrates.

3.4.7 Metabolic engineering

In the post-genomic era, metabolic engineering has made significant advancements with the aid of genome-scale metabolic network models (GEMs) (Fig. 9B), which represent cellular metabolism mathematically and encompass known chemical reactions, metabolites, associated genes (Orth et al., 2010; Thiele and Palsson, 2010). GEMs can be refined and enhanced through the integration of multi-omics data such as transcriptomics (Colijn et al., 2009; Jensen and Papin, 2011; O'Brien et al., 2013; Ravi and Gunawan, 2021), proteomics (Chen et al., 2021; Dahal et al., 2020; Yizhak et al., 2010), and metabolomics (Filippo et al., 2022; Siddiqui et al., 2018; Yizhak et al., 2010). GEMs have been established as a standard platform for analyzing *E. coli*'s metabolism (Fang et al., 2020), and numerous studies have utilized these models for the engineering of *E. coli* to enhance the production of bioproducts.

Guided by GEMs, *E. coli* was successfully engineered to improve anaerobic functionality of the oxidative tricarboxylic acid cycle, thereby effectively generated the necessary reducing power to facilitate the biosynthesis of 1,4-butanediol (Yim et al., 2011). The flux of central and aromatic amino acid biosynthesis reactions was predicted by in silico response analysis of *E. coli* GEM (Yang et al., 2018), which showed a negative correlation between flux and the synthesis rate of D-phenyllactic acid. And knocking them out could enhance the production of aromatic polymers involving D-phenyllactic acid as a monomer.

669 Metabolic modifications had been used in some indigo biosynthesis research (Berry
670 et al., 2002). However, there is still much potential for the utilization of GEMs in indigo
671 and indirubin biosynthesis. This could lead to a more rational approach to metabolic
672 engineering and further enhance the yield of these valuable compounds.
673
674 **3.4.8 Fermentation engineering**
675 Modern fermentation engineering integrates novel technologies such as fermentation
676 process optimization, amplification, and precise control technology with traditional
677 fermentation engineering, which magnificently improve the production. Optimization of
678 composition in culture medium and coenzyme recycle is attempts to increase production
679 of indigo aside from the endeavor in metabolic engineering.
680 The toxicity of indole has been shown to decrease indigo production of the
681 producer microorganisms (Murdock et al., 1993; O'Connor et al., 1997). To address this
682 issue, a two-phase culture system was constructed comprising organic solvent-tolerant
683 microorganisms and non-aqueous media, which enriched indole in the hydrophobic
684 organic solvent and reduced its concentration in the medium (Fig. 9C) (Doukyu et al.,
685 2003). Methyl tert-butyl ether and cyclopentyl methyl ether have been found to be the
686 best organic media for a type II flavin-containing monooxygenase (FMO-E) catalysis
687 and a horse liver alcohol dehydrogenase (HLADH) mediated NADPH regeneration
688 (Huang et al., 2019). Coenzyme regeneration systems have also been designed to

recycle NAD(P)H when applying FMOs in non-aqueous media (Doukyu et al., 2003; Huang et al., 2019).

Following cloning mFMO, the production of bio-indigo was optimized using a response surface methodology with a two-level central composite design to demonstrate the interactions between different pairs in the following three factors: tryptophan, yeast extract and sodium chloride, resulting in a 575% increase in production (Han et al., 2008). Large-scale fermentations were also conducted to validate the application potential of FMOs (Han et al., 2011).

----------**Fig 9**----------

4. The role of FMO in health and disease

TMA is a volatile tertiary amine derived from daily diet. It is primarily produced in the colon, absorbed into the bloodstream, and converted into trimethylamine oxide (TMAO) in the liver by hFMO3 (Fennema et al., 2016). FMO deficiency or excessive TMAO production is associated with various chronic diseases, such as kidney and coronary artery diseases. FMO plays a crucial role in TMA oxidation and is therefore considered a potential therapeutic target for these diseases.

Trimethylaminuria (TMAU) is a genetic disorder caused by a defect in hFMO3. Individuals affected by TMAU have a severely reduced ability to convert TMA into

TMAO, leading to the accumulated TMA that is excreted through sweat, breath, urine, and other bodily fluids. This causes an unpleasant odor resembling rotten fish (Schmidt and Leroux, 2020), which can harm individuals' psychological well-being. Gene therapy targeting hFMO3 is a promising method for treating TMAU, but limited research data is available (Donato et al., 2021). Additionally, detecting hFMO3 mutations is critical for diagnosing TMAU and expanding the corresponding gene mutation data to promote functional genomics research and explain the disease's pathogenesis. Despite numerous sequencing studies on samples of TMAU worldwide, there is limited research on the association between mutations and the loss of function of hFMO3 (Ameria et al., 2015). In 2021, modeling analysis and experimental verifications were conducted on some hFMO3 mutations considered to be polymorphic or benign. The results suggested that these mutations might damage FMO dynamics, but the causal relationship between these mutations and the pathogenic mechanism could not be confirmed.

TMAO is an atherogenic metabolite that affects platelet reactivity and thrombosis potential. Excessive TMAO production can impose a burden on the cardiovascular system (Janeiro et al., 2018; Senthong et al., 2016; Tang et al., 2019; Xu and Yang, 2021). Targeting metabolic pathways associated with TMAO may be a feasible method for treating atherosclerosis (Yang et al., 2019). TMAO has become an essential pathogenic factor and therapeutic target for treating coronary heart disease. Recent studies have shown that skin fibroblasts, vascular endothelial cells, and adipocyte

progenitors are reprogrammed into myofibroblasts through the TMA-FMO-TMAO-PERK pathway, leading to systemic sclerosis syndrome caused by intestinal dysregulation (Kim et al., 2022). hFMO3, the key enzyme in this pathway, is a potential therapeutic target for specific regulation of its association with upstream chemicals (Zhu et al., 2018).

5. Conclusions

The studies related to FMOs and biosynthesis have a long history, spanning over 50 years since the discovery of FMO from pig liver in 1972. The emergence of indigo biosynthesis was in 1989. And the first report of indigo biosynthesis by mFMO was published in 2003. FMOs exhibit some variations across species. In human, hFMOs are located at the ER of hepatocytes towards the cytoplasm, while in bacteria, mFMO is water-soluble. The structures and catalytic mechanisms of FMOs have been extensively studied, and FMOs are increasingly recognized for their crucial roles in biosynthesis, biosensors, diseases, and drug metabolism due to the broad substrate specificity. New biotechnologies, such as directed evolution, *de novo* design, and GEMs, can be used to further improve the yield of FMOs. However, there are still many challenges and questions that need to be addressed. This review aims to provide insights to scientists, who can use this information to further explore the potential of FMOs in various fields.

Abbreviations

AncFMO: ancient mammalian FMO

ArBVMO: BVMO cloned from *Acinetobacter radioresistens*

bFMO: FMO cloned from *Methylophaga aminisulfidivorans*

BVMOs: baeyer-villiger monooxygenases

CFA: cyclopropane fatty acid

cFMO: FMO cloned from *Corynebacterium glutamicum*

CHMOs: cyclohexanone monooxygenases

CYP450: cytochrome P450

DDAB: didodecylammonium bromide

DDPMs: denoising diffusion probabilistic models

DMS: dimethylsulfate

DMSO: dimethylsulfoxide

DTME: dithio-bismaleimidoethane

ER: endoplasmic reticulum

FAD: flavin adenine dinucleotide

FMOs: flavin-containing monooxygenases

FMO-E: type II flavin-containing monooxygenase cloned from *Rhodococcus jostii* RHA1

FMO6p: flavin containing dimethylaniline monoxygenase 6, pseudogene

FPMOs: flavoprotein monooxygenases

GC: glassy carbon

GEMs: genome-scale metabolic network models

hFMO: human flavin-containing monooxygenase

HLADH: horse liver alcohol dehydrogenase

IAA: indole-3-acetic acid

IPyA: indole-3-pyruvate acid

ITCHY: incremental truncation for the creation of hybrid enzymes

MaSIF: molecular surface interaction fingerprinting

MBP: maltose-binding protein

MC: monte carlo

MCMC: markov chain monte carlo

mFMO: FMO cloned from *Methylophaga sp.* strain SK1

MPNN: message-passing neural network

MSA: multiple sequence alignment

NADPH: nicotinamide adenine dinucleotide phosphate

NiFMO: FMO cloned from *Nitrincola lacisaponensis*

NMOs: N-hydroxylating monooxygenases

pFMO: pig flavin-containing monooxygenase

PROSS: protein repair one-stop shop

PTDH: phosphate dehydrogenase

PtFMO: FMO cloned from *Polygonum tinctorium*

RACHITT: random chimeragenesis on transient templates

rFMO: rabbit FMO

rmFMO: FMO cloned from *rhesus macaque*

RM-PCR: random multi-recombinant PCR

RPR: random priming *in vitro* recombination

RRI: residue-residue interaction

SHIPREC: sequence homology-independent protein recombination

SMFMO: FMO cloned from *S. maltophilia*

SMO: styrene monooxygenase

SNPs: single nucleotide polymorphic variants

StEP: staggered extension process

TMA: trimethylamine

TMAO: trimethylamine oxide

TMAU: trimethylaminuria

TMM: trimethylamine monooxygenase

TRP: tryptophanase

UPO: unspecific peroxygenase

6BrIG: 6,6'-dibromoindigo

CRediT authorship contribution statement

Changxin Fan: Conceptualization, Formal analysis, Investigation, Writing - Original Draft, Writing - Review & Editing, Visualization. **Ziqi Xie**: Conceptualization, Investigation, Writing - Original Draft, Writing - Review & Editing, Visualization. **Yijin Li**: Investigation, Writing - Original Draft, Visualization. **Ruihan Zhang**: Investigation, Writing - Original Draft. **Da Zheng**: Formal analysis, Investigation, Writing - Original Draft, Visualization. **Jiacheng Shi**: Investigation, Writing - Original Draft. **Yifei Wang**: Investigation, Writing - Original Draft. **Mingyuan Cheng**: Visualization. **Yu Zhou**: Supervision. **Yi Zhan**: Supervision, Project administration, Writing - Original Draft. **Yunjun Yan**: Project administration, Writing - Review & Editing, Funding acquisition.

Acknowledgements

We thank dockeasy.cn, biorender.com, and scidraw.io for illustrations. This work was supported by the National Funding for Undergraduate Innovation and Entrepreneurship Training of China (No.202210487002).

825 **References**

826 Abraham, M.J., Murtola, T., Schulz, R., Páll, S., Smith, J.C., Hess, B., Lindahl, E., 2015.
827 GROMACS: High performance molecular simulations through multi-level parallelism
828 from laptops to supercomputers. SoftwareX 1-2, 19-25.

829 Alfieri, A., Malito, E., Orru, R., Fraaije, M.W., Mattevi, A., 2008. Revealing the
830 moonlighting role of NADP in the structure of a flavin-containing monooxygenase.
831 PNAS 105 (18), 6572-6577.

832 Ameria, S.P., Jung, H.S., Kim, H.S., Han, S.S., Kim, H.S., Lee, J.H., 2015.
833 Characterization of a flavin-containing monooxygenase from *Corynebacterium*
834 *glutamicum* and its application to production of indigo and indirubin. Biotechnol. Lett.
835 37 (8), 1637-1644.

836 Anishchenko, I., Pellock, S.J., Chidyausiku, T.M., Ramelot, T.A., Ovchinnikov, S., Hao,
837 J., Bafna, K., Norn, C., Kang, A., Bera, A.K., DiMaio, F., Carter, L., Chow, C.M.,
838 Montelione, G.T., Baker, D., 2021. *De novo* protein design by deep network
839 hallucination. Nature 600 (7889), 547-552.

840 Ball, S., Bruice, T.C., 1980. Oxidation of amines by a 4a-hydroperoxyflavin. J. Am.
841 Chem. Soc. 102 (21), 6498-6503.

842 Beaty, N.B., Ballou, D.P., 1981a. The oxidative half-reaction of liver microsomal
843 FAD-containing monooxygenase. J. Biol. Chem. 256 (9), 4619-4625.

844 Beaty, N.B., Ballou, D.P., 1981b. The reductive half-reaction of liver microsomal

845 FAD-containing monooxygenase. J. Biol. Chem. 256 (9), 4611-4618.
846 Beier, A., Bordewick, S., Genz, M., Schmidt, S., van den Bergh, T., Peters, C., Joosten,
847 H.-J., Bornscheuer, U.T., 2016. Switch in cofactor specificity of a Baeyer‐Villiger
848 monooxygenase. ChemBioChem 17 (24), 2312-2315.
849 Berry, A., Dodge, T.C., Pepsin, M., Weyler, W., 2002. Application of metabolic
850 engineering to improve both the production and use of biotech indigo. J. Ind. Microbiol.
851 Biotechnol. 28 (3), 127-133.
852 Biradar, A.A., Biradar, A.V., Asefa, T., 2010. Entrapping flavin-containing
853 monooxygenase on corrugated silica nanospheres and their recyclable biocatalytic
854 activities. ChemCatChem 2 (8), 1004-1010.
855 Boronin, A., Tsoĭ, T., Kosheleva, I., Arinbasarov, M., Adanin, V., 1989. Cloning of
856 Pseudomonas putida genes responsible for the primary stages of oxidation of
857 naphthalene in Escherichia coli cells. Genetika 25 (2), 226-237.
858 Bortolussi, S., Catucci, G., Gilardi, G., Sadeghi, S.J., 2021. N- and S-oxygenation
859 activity of truncated human flavin-containing monooxygenase 3 and its common
860 polymorphic variants. Arch. Biochem. Biophys. 697, 108663.
861 Boyken, S.E., Chen, Z., Groves, B., Langan, R.A., Oberdorfer, G., Ford, A., Gilmore,
862 J.M., Xu, C., DiMaio, F., Pereira, J.H., Sankaran, B., Seelig, G., Zwart, P.H., Baker, D.,
863 2016. De novo design of protein homo-oligomers with modular hydrogen-bond
864 network–mediated specificity. Science 352 (6286), 680-687.

865 Burnett, V.L., Lawton, M.P., Philpot, R.M., 1994. Cloning and sequencing of
866 flavin-containing monooxygenases FMO_3 and FMO_4 from rabbit and characterization of
867 FMO3. J. Biol. Chem. 269 (19), 14314-14322.
868 Cadwell, R.C., Joyce, G.F., 1992. Randomization of genes by PCR mutagenesis. PCR
869 Meth. Appl. 2 (1), 28-33.
870 Cahn, J.K.B., Brinkmann-Chen, S., Arnold, F.H., 2018. Enzyme Nicotinamide Cofactor
871 Specificity Reversal Guided by Automated Structural Analysis and Library Design, in:
872 Jensen, M.K., Keasling, J.D. (Eds.), Synthetic Metabolic Pathways: Methods and
873 Protocols. Springer New York, New York, pp. 15-26.
874 Cao, X., Yang, H., Shang, C., Ma, S., Liu, L., Cheng, J., 2019. The roles of auxin
875 biosynthesis YUCCA gene family in plants. Int. J. Mol. Sci. 20 (24), 6343.
876 Cashman, J.R., Akerman, B.R., Forrest, S.M., Treacy, E.P., 2000. Population-specific
877 polymorphisms of the humanFMO_3 gene: Significance for detoxication. Drug Metab.
878 Dispos. 28 (2), 169-173.
879 Castrignanò, S., Gilardi, G., Sadeghi, S.J., 2015. Human flavin-containing
880 monooxygenase 3 on graphene oxide for drug metabolism screening. Anal. Chem. 87
881 (5), 2974-2980.
882 Castrignanò, S., Sadeghi, S.J., Gilardi, G., 2010. Electro-catalysis by immobilised
883 human flavin-containing monooxygenase isoform 3 (hFMO3). Anal. Bioanal. Chem.
884 398 (3), 1403-1409.

885 Catucci, G., Aramini, D., Sadeghi, S.J., Gilardi, G., 2020. Ligand stabilization and effect
886 on unfolding by polymorphism in human flavin-containing monooxygenase 3. Int. J.
887 Biol. Macromol. 162, 1484-1493.
888 Catucci, G., Gao, C., Sadeghi, S.J., Gilardi, G., 2017. Chemical applications of Class B
889 flavoprotein monooxygenases. Rend. Lincei-Sci. Fis. Nat. 28, 195-206.
890 Catucci, G., Turella, S., Cheropkina, H., De Angelis, M., Gilardi, G., Sadeghi, S.J., 2022.
891 Green production of indigo and indirubin by an engineered Baeyer–Villiger
892 monooxygenase. Biocatal. Agric. Biotechnol. 44, 102458.
893 Ceccoli, R.D., Bianchi, D.A., Rial, D.V., 2014. Flavoprotein monooxygenases for
894 oxidative biocatalysis: recombinant expression in microbial hosts and applications.
895 Front. Microbiol. 5, 25.
896 Chen, H., Ma, L., Dai, H., Fu, Y., Wang, H., Zhang, Y., 2022. Advances in rational
897 protein engineering toward functional architectures and their applications in food
898 science. J. Agric. Food Chem. 70 (15), 4522-4533.
899 Chen, M., Guan, B., Xu, H., Yu, F., Zhang, T., Wu, B., 2019. The molecular mechanism
900 regulating diurnal rhythm of flavin-containing monooxygenase 5 in mouse liver. Drug
901 Metab. Dispos. 47 (11), 1333-1342.
902 Chen, T., Wang, X., Zhuang, L., Shao, A., Lu, Y., Zhang, H., 2021. Development and
903 optimization of a microbial co-culture system for heterologous indigo biosynthesis.
904 Microb. Cell Fact. 20 (1), 1-11.

Chen, Y., Patel, N.A., Crombie, A., Scrivens, J.H., Murrell, J.C., 2011. Bacterial flavin-containing monooxygenase is trimethylamine monooxygenase. PNAS 108 (43), 17791-17796.

Chen, Y., Pelt‐KleinJan, E., Olst, B., Douwenga, S., Boeren, S., Bachmann, H., Molenaar, D., Nielsen, J., Teusink, B., 2021. Proteome constraints reveal targets for improving microbial fitness in nutrient‐rich environments. Mol. Syst. Biol. 17 (4), e10093.

Cheng, L., Yin, S., Chen, M., Sun, B., Hao, S., Wang, C., 2016. Enhancing indigo production by over-expression of the styrene monooxygenase in *Pseudomonas putida*. Curr. Microbiol. 73 (2), 248-254.

Cherrington, N.J., Cao, Y., Cherrington, J.W., Rose, R.L., Hodgson, E., 1998. Physiological factors affecting protein expression of flavin-containing monooxygenases 1, 3 and 5. Xenobiotica 28 (7), 673-682.

Cho, D.H., Kim, H.J., Oh, S.J., Hwang, J.H., Shin, N., Bhatia, S.K., Yoon, J.J., Jeon, J.M., Yang, Y.H., 2023. Strategy for efficiently utilizing *Escherichia coli* cells producing isobutanol by combining isobutanol and indigo production systems. J. Biotechnol. 367, 62-70.

Cho, H.J., Cho, H.Y., Kim, K.J., Kim, M.H., Kim, S.W., Kang, B.S., 2011. Structural and functional analysis of bacterial flavin-containing monooxygenase reveals its ping-pong-type reaction mechanism. J. Struct. Biol. 175 (1), 39-48.

925 Choi, H.S., Kim, J.K., Cho, E.H., Kim, Y.C., Kim, J.I., Kim, S.W., 2003. A novel
926 flavin-containing monooxygenase from *Methylophaga* sp. strain SK1 and its indigo
927 synthesis in *Escherichia coli*. Biochem. Biophys. Res. Commun. 306 (4), 930-936.
928 Choi, K.Y., 2020. A review of recent progress in the synthesis of bio-indigoids and their
929 biologically assisted end-use applications. Dyes Pigm. 181, 108570.
930 Chowdhury, R., Maranas, C.D., 2020. From directed evolution to computational enzyme
931 engineering—A review. AIChE J. 66 (3), e16847.
932 Coco, W.M., 2003. RACHITT: Gene family shuffling by Random Chimeragenesis on
933 transient templates. Methods Mol. Biol. 231, 111-127.
934 Colijn, C., Brandes, A., Zucker, J., Lun, D.S., Weiner, B., Farhat, M.R., Cheng, T.-Y.,
935 Moody, D.B., Murray, M., Galagan, J.E., 2009. Interpreting expression data with
936 metabolic flux models: Predicting *Mycobacterium tuberculosis* mycolic acid production.
937 PLoS Comput. Biol. 5 (8), e1000489.
938 Dahal, S., Yurkovich, J.T., Xu, H., Palsson, B.O., Yang, L., 2020. Synthesizing systems
939 biology knowledge from omics using genome‐scale models. Proteomics 20 (17-18),
940 1900282.
941 Dai, C., Ma, Q., Li, Y., Zhou, D., Yang, B., Qu, Y., 2019. Application of an efficient
942 indole oxygenase system from Cupriavidus sp. SHE for indigo production. Bioprocess
943 Biosyst. Eng. 42, 1963-1971.
944 Dauparas, J., Anishchenko, I., Bennett, N., Bai, H., Ragotte, R.J., Milles, L.F., Wicky,

945 B.I.M., Courbet, A., de Haas, R.J., Bethel, N., Leung, P.J.Y., Huddy, T.F., Pellock, S.,
946 Tischer, D., Chan, F., Koepnick, B., Nguyen, H., Kang, A., Sankaran, B., Bera, A.K.,
947 King, N.P., Baker, D., 2022. Robust deep learning–based protein sequence design using
948 ProteinMPNN. Science 378 (6615), 49-56.
949 Davey, J.A., Damry, A.M., Goto, N.K., Chica, R.A., 2017. Rational design of proteins
950 that exchange on functional timescales. Nat. Chem. Biol. 13 (12), 1280-1285.
951 Dehouck, Y., Kwasigroch, J.M., Gilis, D., Rooman, M., 2011. PoPMuSiC 2.1: a web
952 server for the estimation of protein stability changes upon mutation and sequence
953 optimality. BMC Bioinform. 12 (1), 151.
954 Ding, W., Nakai, K., Gong, H., 2022. Protein design via deep learning. Brief. Bioinform.
955 23 (3), bbac102.
956 Dolphin, C.T., Cullingford, T.E., Shephard, E.A., Smith, R.L., Phillips, I.R., 1996.
957 Differential developmental and tissue-specific regulation of expression of the genes
958 encoding three members of the flavin-containing monooxygenase family of man, FMO1,
959 FMO3 and FM04. Eur. J. Biochem. 235 (3), 683-689.
960 Donato, L., Alibrandi, S., Scimone, C., Castagnetti, A., Rao, G., Sidoti, A., D'Angelo,
961 R., 2021. Gut-brain axis cross-talk and limbic disorders as biological basis of secondary
962 TMAU. J. Pers. Med. 11 (2), 87.
963 Doukyu, N., Nakano, T., Okuyama, Y., Aono, R., 2002. Isolation of an *Acinetobacter* sp.
964 ST-550 which produces a high level of indigo in a water-organic solvent two-phase

965 system containing high levels of indole. Appl. Microbiol. Biotechnol. 58 (4), 543-546.
966 Doukyu, N., Toyoda, K., Aono, R., 2003. Indigo production by *Escherichia coli*
967 carrying the phenol hydroxylase gene from *Acinetobacter* sp. strain ST-550 in a
968 water-organic solvent two-phase system. Appl. Microbiol. Biotechnol. 60 (6), 720-725.
969 Du, J., Yang, D., Luo, Z.W., Lee, S.Y., 2018. Metabolic engineering of *Escherichia coli*
970 for the production of indirubin from glucose. J. Biotechnol. 267, 19-28.
971 Eastman, P., Swails, J., Chodera, J.D., McGibbon, R.T., Zhao, Y.T., Beauchamp, K.A.,
972 Wang, L.P., Simmonett, A.C., Harrigan, M.P., Stern, C.D., Wiewiora, R.P., Brooks, B.R.,
973 Pande, V.S., 2017. OpenMM 7: Rapid development of high performance algorithms for
974 molecular dynamics. PLoS Comput. Biol. 13 (7), e1005659.
975 Ensley, B.D., Ratzkin, B.J., Osslund, T.D., Simon, M.J., Wackett, L.P., Gibson, D.T.,
976 1983. Expression of naphthalene oxidation genes in Escherichia coli results in the
977 biosynthesis of indigo. Science 222 (4620), 167-169.
978 Eswaramoorthy, S., Bonanno, J.B., Burley, S.K., Swaminathan, S., 2006. Mechanism of
979 action of a flavin-containing monooxygenase. PNAS 103 (26), 9832-9837.
980 Fabara, A.N., Fraaije, M.W., 2020. An overview of microbial indigo-forming enzymes.
981 Appl. Microbiol. Biotechnol. 104 (3), 925-933.
982 Fabara, A.N., Fraaije, M.W., 2020. Production of indigo through the use of a
983 dual-function substrate and a bifunctional fusion enzyme. Enzyme Microb. Technol. 142,
984 109692.

985 Fang, X., Lloyd, C.J., Palsson, B.O., 2020. Reconstructing organisms in silico:
986 genome-scale models and their emerging applications. Nat. Rev. Microbiol. 18 (12),
987 731-743.
988 Fennema, D., Phillips, I.R., Shephard, E.A., 2016. Trimethylamine and trimethylamine
989 N-oxide, a flavin-containing monooxygenase 3 (FMO3)-mediated host-microbiome
990 metabolic axis implicated in health and disease. Drug Metab. Dispos. 44 (11),
991 1839-1850.
992 Ferreira, P., Fernandes, P.A., Ramos, M.J., 2022. Modern computational methods for
993 rational enzyme engineering. Chem Catal. 2 (10), 2481-2498.
994 Ferrero, V.E.V., Andolfi, L., Di Nardo, G., Sadeghi, S.J., Fantuzzi, A., Cannistraro, S.,
995 Gilardi, G., 2008. Protein and electrode engineering for the covalent immobilization of
996 P450 BMP on gold. Anal. Chem. 80 (22), 8438-8446.
997 Ferruz, N., Schmidt, S., Höcker, B., 2022. ProtGPT2 is a deep unsupervised language
998 model for protein design. Nat. Commun. 13 (1), 4348.
999 Filippo, M.D., Pescini, D., Galuzzi, B.G., Bonanomi, M., Gaglio, D., Mangano, E.,
1000 Consolandi, C., Alberghina, L., Vanoni, M., Damiani, C., 2022. INTEGRATE:
1001 Model-based multi-omics data integration to characterize multi-level metabolic
1002 regulation. PLoS Comput. Biol. 18 (2), e1009337.
1003 Fiorentini, F., Hatzl, A.-M., Schmidt, S., Savino, S., Glieder, A., Mattevi, A., 2018. The
1004 extreme structural plasticity in the CYP153 subfamily of P450s directs development of

designer hydroxylases. Biochemistry 57 (48), 6701-6714.

Furnes, B., Schlenk, D., 2004. Evaluation of xenobiotic N-and S-oxidation by variant flavin-containing monooxygenase 1 (FMO1) enzymes. Toxicol. Sci. 78 (2), 196-203.

Fürst, M.J.L.J., Boonstra, M., Bandstra, S., Fraaije, M.W., 2019a. Stabilization of cyclohexanone monooxygenase by computational and experimental library design. Biotechnol. Bioeng. 116 (9), 2167-2177.

Fürst, M.J.L.J., Fiorentini, F., Fraaije, M.W., 2019b. Beyond active site residues: overall structural dynamics control catalysis in flavin-containing and heme-containing monooxygenases. Curr. Opin. Struct. Biol. 59, 29-37.

Gainza, P., Wehrle, S., Van Hall-Beauvais, A., Marchand, A., Scheck, A., Harteveld, Z., Buckley, S., Ni, D., Tan, S., Sverrisson, F., Goverde, C., Turelli, P., Raclot, C., Teslenko, A., Pacesa, M., Rosset, S., Georgeon, S., Marsden, J., Petruzzella, A., Liu, K., Xu, Z., Chai, Y., Han, P., Gao, G.F., Oricchio, E., Fierz, B., Trono, D., Stahlberg, H., Bronstein, M., Correia, B.E., 2023. *De novo* design of protein interactions with learned surface fingerprints. Nature 617 (7959), 176-184.

Gao, C., Catucci, G., Di Nardo, G., Gilardi, G., Sadeghi, S.J., 2016. Human flavin-containing monooxygenase 3: Structural mapping of gene polymorphisms and insights into molecular basis of drug binding. Gene 593 (1), 91-99.

Gao, C., Zheng, T., 2019. Drug metabolite synthesis by immobilized human FMO_3 and whole cell catalysts. Microb. Cell Fact. 18 (1), 133.

1025 Goldenzweig, A., Goldsmith, M., Hill, S.E., Gertman, O., Laurino, P., Ashani, Y., Dym,
1026 O., Unger, T., Albeck, S., Prilusky, J., Lieberman, R.L., Aharoni, A., Silman, I.,
1027 Sussman, J.L., Tawfik, D.S., Fleishman, S.J., 2016. Automated structure- and
1028 sequence-based design of proteins for high bacterial expression and stability. Mol. Cell.
1029 63 (2), 337-346.
1030 Gonzalez-Perez, D., Garcia-Ruiz, E., Ruiz-Dueñas, F.J., Martinez, A.T., Alcalde, M.,
1031 2014. Structural determinants of oxidative stabilization in an evolved versatile
1032 peroxidase. ACS Catal. 4 (11), 3891-3901.
1033 Goodsell, D.S., Sanner, M.F., Olson, A.J., Forli, S., 2021. The Auto Docksuite at 30.
1034 Protein Sci. 30 (1), 31-43.
1035 Goris, M., Cea-Rama, I., Puntervoll, P., Ree, R., Almendral, D., Sanz-Aparicio, J.,
1036 Ferrer, M., Bjerga, G.E.K., 2023. Increased thermostability of an engineered
1037 flavin-containing monooxygenase to remediate trimethylamine in fish protein
1038 hydrolysates. Appl. Environ. Microbiol. 89 (6), e00390-23.
1039 Groeneveld, M., Van Beek, H., Duetz, W., Fraaije, M., 2016. Identification of a novel
1040 oxygenase capable of regiospecific hydroxylation of D-limonene into (+)-trans-carveol.
1041 Tetrahedron 72 (46), 7263-7267.
1042 Guffy, S.L., Teets, F.D., Langlois, M.I., Kuhlman, B., 2018. Protocols for
1043 requirement-driven protein design in the rosetta modeling program. J. Chem. Inf. Model.
1044 58 (5), 895-901.

1045 Hallen, M.A., Martin, J.W., Ojewole, A., Jou, J.D., Lowegard, A.U., Frenkel, M.S.,
1046 Gainza, P., Nisonoff, H.M., Mukund, A., Wang, S.Y., Holt, G.T., Zhou, D., Dowd, E.,
1047 Donald, B.R., 2018. OSPREY 3.0: Open-source protein redesign for you, with powerful
1048 new features. J. Comput. Chem. 39 (30), 2494-2507.
1049 Ham, S., Cho, D.-H., Oh, S.J., Hwang, J.H., Kim, H.J., Shin, N., Ahn, J., Choi, K.-Y.,
1050 Bhatia, S.K., Yang, Y.-H., 2023. Enhanced production of bio-indigo in engineered
1051 *Escherichia coli*, reinforced by cyclopropane-fatty acid-acyl-phospholipid synthase
1052 from psychrophilic Pseudomonas sp. B14-6. J. Biotechnol. 366, 1-9.
1053 Han, A., Robinson, R.M., Badieyan, S., Ellerbrock, J., Sobrado, P., 2013. Tryptophan-47
1054 in the active site of *Methylophaga* sp. strain SK1 flavin-monooxygenase is important for
1055 hydride transfer. Arch. Biochem. Biophys. 532 (1), 46-53.
1056 Han, G.H., Bang, S.E., Babu, B.K., Chang, M., Shin, H.J., Kim, S.W., 2011. Bio-indigo
1057 production in two different fermentation systems using recombinant *Escherichia coli*
1058 cells harboring a flavin-containing monooxygenase gene (fmo). Process Biochem. 46
1059 (3), 788-791.
1060 Han, G.H., Gim, G.H., Kim, W., Seo, S.I., Kim, S.W., 2012. Enhanced indirubin
1061 production in recombinant *Escherichia coli* harboring a flavin-containing
1062 monooxygenase gene by cysteine supplementation. J. Biotechnol. 164 (2), 179-187.
1063 Han, G.H., Shin, H.J., Kim, S.W., 2008. Optimization of bio-indigo production by
1064 recombinant *E. coli* harboring fmo gene. Enzyme Microb. Technol. 42 (7), 617-623.

1065 Hao, D.C., Chen, S.L., Mu, J., Xiao, P.G., 2009. Molecular phylogeny, long-term
1066 evolution, and functional divergence of flavin-containing monooxygenases. Genetica
1067 137 (2), 173-187.
1068 Harteveld, Z., Bonet, J., Rosset, S., Yang, C., Sesterhenn, F., Correia, B.E., 2022. A
1069 generic framework for hierarchical *de novo* protein design. PNAS 119 (43),
1070 e2206111119.
1071 Henderson, M.C., Krueger, S.K., Siddens, L.K., Stevens, J.F., Williams, D.E., 2004.
1072 S-oxygenation of the thioether organophosphate insecticides phorate and disulfoton by
1073 human lung flavin-containing monooxygenase 2. Biochem. Pharmacol. 68 (5), 959-967.
1074 Hernandez, D., Janmohamed, A., Chandan, P., Phillips, I.R., Shephard, E.A., 2004.
1075 Organization and evolution of the flavin-containing monooxygenase genes of human
1076 and mouse: identification of novel gene and pseudogene clusters. Pharmacogenetics 14
1077 (2), 117-130.
1078 Honda, K., Yamashita, S., Nakagawa, H., Sameshima, Y., Omasa, T., Kato, J., Ohtake,
1079 H., 2008. Stabilization of water-in-oil emulsion by *Rhodococcus opacus* B-4 and its
1080 application to biotransformation. Appl. Microbiol. Biotechnol. 78 (5), 767-773.
1081 Hsu, T.M., Welner, D.H., Russ, Z.N., Cervantes, B., Prathuri, R.L., Adams, P.D., Dueber,
1082 J.E., 2018. Employing a biochemical protecting group for a sustainable indigo dyeing
1083 strategy. Nat. Chem. Biol. 14 (3), 256-261.
1084 Hu, W.S., Bowman, E.H., Delviks, K.A., Pathak, V.K., 1997. Homologous

recombination occurs in a distinct retroviral subpopulation and exhibits high negative interference. J. Virol. 71 (8), 6028-6036.

Huang, L., Aalbers, F.S., Tang, W., Röllig, R., Fraaije, M.W., Kara, S., 2019. Convergent cascade catalyzed by monooxygenase–alcohol dehydrogenase fusion applied in organic media. ChemBioChem 20 (13), 1653-1658.

Jung, H.S., Jung, H.B., Kim, H.S., Kim, C.G., Lee, J.H., 2018. Protein engineering of flavin-containing monooxygenase from *Corynebacterium glutamicum* for improved production of indigo and indirubin. Korean Soc. Life Sci. 28 (6), 656-662.

Inoue, S., Morita, R., Minami, Y., 2021. An indigo-producing plant, *Polygonum tinctorium*, possesses a flavin containing monooxygenase capable of oxidizing indole. Biochem. Biophys. Res. Commun. 543, 95.

Jain, A.N., 2003. Surflex: Fully Automatic Flexible molecular docking using a molecular similarity-based search engine. J. Med. Chem. 46 (4), 499-511.

Janeiro, M.H., Ramírez, M.J., Milagro, F.I., Martínez, J.A., Solas, M., 2018. Implication of trimethylamine n-oxide (TMAO) in disease: Potential biomarker or new therapeutic target. Nutrients 10 (10), 1398.

Janmohamed, A., Hernandez, D., Phillips, I.R., Shephard, E.A., 2004. Cell-, tissue-, sex- and developmental stage-specific expression of mouse flavin-containing monooxygenases (Fmos). Biochem. Pharmacol. 68 (1), 73-83.

Jensen, C.N., Cartwright, J., Ward, J., Hart, S., Turkenburg, J.P., Ali, S.T., Allen, M.J.,

Grogan, G., 2012. A flavoprotein monooxygenase that catalyses a Baeyer-Villiger reaction and thioether oxidation using NADH as the nicotinamide cofactor. ChemBioChem 13 (6), 872-878.

Jensen, P.A., Papin, J.A., 2011. Functional integration of a metabolic network model and expression data without arbitrary thresholding. Bioinformatics 27 (4), 541-547.

Jia, L., Lu, W., Hu, D., Feng, M., Wang, A., Wang, R., Sun, H., Wang, P., Xia, Q., Ma, S., 2023. Genetically engineered blue silkworm capable of synthesizing natural blue pigment. Int. J. Biol. Macromol. 235, 123863.

Jumper, J., Evans, R., Pritzel, A., Green, T., Figurnov, M., Ronneberger, O., Tunyasuvunakool, K., Bates, R., Zidek, A., Potapenko, A., Bridgland, A., Meyer, C., Kohl, S.A.A., Ballard, A.J., Cowie, A., Romera-Paredes, B., Nikolov, S., Jain, R., Adler, J., Back, T., Petersen, S., Reiman, D., Clancy, E., Zielinski, M., Steinegger, M., Pacholska, M., Berghammer, T., Bodenstein, S., Silver, D., Vinyals, O., Senior, A.W., Kavukcuoglu, K., Kohli, P., Hassabis, D., 2021. Highly accurate protein structure prediction with AlphaFold. Nature 596 (7873), 583-589.

Kalmankar, N.V., Pavalam, M., Indrakumar, S., Srinivasan, N., Sowdhamini, R., 2022. DSDBASE 2.0: updated version of DiSulphide dataBASE, a database on disulphide bonds in proteins. Database 2022, baac005.

Kikuchi, M., Ohnishi, K., Harayama, S., 2000. An effective family shuffling method using single-stranded DNA. Gene 243 (1), 133-137.

Kim, J., Lee, J., Lee, P.G., Kim, E.J., Kroutil, W., Kim, B.G., 2019. Elucidating cysteine-assisted synthesis of indirubin by a flavin-containing monooxygenase. ACS Catal. 9 (10), 9539-9544.

Kim, J., Lee, P.-g., Jung, E.-o., Kim, B.-G., 2018. In vitro characterization of CYP102G4 from *Streptomyces cattleya*: A self-sufficient P450 naturally producing indigo. BBA-Proteins Proteom. 1866 (1), 60-67.

Kim, J., Park, S., Min, D., Kim, W., 2021. Comprehensive survey of recent drug discovery using deep learning. Int. J. Mol. Sci. 22 (18).

Kim, S.J., Bale, S., Verma, P., Wan, Q., Ma, F., Gudjonsson, J.E., Hazen, S.L., Harms, P.W., Tsou, P.S., Khanna, D., Tsoi, L.C., Gupta, N., Ho, K.J., Varga, J., 2022. Gut microbe-derived metabolite trimethylamine N-oxide activates PERK to drive fibrogenic mesenchymal differentiation. iScience 25 (7), 104669.

Krueger, S.K., Martin, S.R., Yueh, M.-F., Pereira, C.B., Williams, D.E., 2002a. Identification of active flavin-containing monooxygenase isoform 2 in human lung and characterization of expressed protein. Drug Metab. Dispos. 30 (1), 34-41.

Krueger, S.K., Williams, D.E., 2005. Mammalian flavin-containing monooxygenases: structure/function, genetic polymorphisms and role in drug metabolism. Pharmacol. Ther. 106 (3), 357-387.

Krueger, S.K., Williams, D.E., Yueh, M.-F., Martin, S.R., Hines, R.N., Raucy, J.L., Dolphin, C.T., Shephard, E.A., Phillips, I.R., 2002b. Genetic polymorphisms of

flavin-containing monooxygenase (FMO). Drug Metab. Rev. 34 (3), 523-532.

Land, H., Humble, M.S., 2018. YASARA: A Tool to Obtain Structural Guidance in Biocatalytic Investigations, in: Bornscheuer, U.T., Höhne, M. (Eds.), Protein Engineering: Methods and Protocols. Springer New York, New York, pp. 43-67.

Larsen-Su, S., Krueger, S.K., Yueh, M.F., Lee, M.Y., Shehin, S.E., Hines, R.N., Williams, D.E., 1999. Flavin-containing monooxygenase isoform 2: developmental expression in fetal and neonatal rabbit lung. J. Biochem. Mol. Toxicol. 13 (3-4), 187-193.

Lattard, V., Longin-Sauvageon, C., Benoit, E., 2003. Cloning, sequencing and tissue distribution of rat flavin-containing monooxygenase 4: two different forms are produced by tissue-specific alternative splicing. Mol. Pharmacol. 63 (1), 253-261.

Lawton, M.P., Cashman, J.R., Cresteil, T., Dolphin, C.T., Elfarra, A.A., Hines, R.N., Hodgson, E., Kimura, T., Ozols, J., Phillips, I.R., Philpot, R.M., Poulsen, L.L., Rettie, A.E., Shephard, E.A., Williams, D.E., Ziegler, D.M., 1994. A nomenclature for the mammalian flavin-containing monooxygenase gene family based on amino acid sequence identities. Arch. Biochem. Biophys. 308 (1), 254-257.

Lee, J., Kim, J., Song, J.E., Song, W.S., Kim, E.J., Kim, Y.G., Jeong, H.J., Kim, H.R., Choi, K.Y., Kim, B.G., 2021. Production of Tyrian purple indigoid dye from tryptophan in *Escherichia coli*. Nat. Chem. Biol. 17 (1), 104-112.

Lee, J.S., Kim, J., Kim, P.M., 2023. Score-based generative modeling for de novo

protein design. Nat. Comput. Sci. 3 (5), 382-392.

Leman, J.K., Weitzner, B.D., Lewis, S.M., Adolf-Bryfogle, J., Alam, N., Alford, R.F., Aprahamian, M., Baker, D., Barlow, K.A., Barth, P., Basanta, B., Bender, B.J., Blacklock, K., Bonet, J., Boyken, S.E., Bradley, P., Bystroff, C., Conway, P., Cooper, S., Correia, B.E., Coventry, B., Das, R., De Jong, R.M., DiMaio, F., Dsilva, L., Dunbrack, R., Ford, A.S., Frenz, B., Fu, D.Y., Geniesse, C., Goldschmidt, L., Gowthaman, R., Gray, J.J., Gront, D., Guffy, S., Horowitz, S., Huang, P.-S., Huber, T., Jacobs, T.M., Jeliazkov, J.R., Johnson, D.K., Kappel, K., Karanicolas, J., Khakzad, H., Khar, K.R., Khare, S.D., Khatib, F., Khramushin, A., King, I.C., Kleffner, R., Koepnick, B., Kortemme, T., Kuenze, G., Kuhlman, B., Kuroda, D., Labonte, J.W., Lai, J.K., Lapidoth, G., Leaver-Fay, A., Lindert, S., Linsky, T., London, N., Lubin, J.H., Lyskov, S., Maguire, J., Malmström, L., Marcos, E., Marcu, O., Marze, N.A., Meiler, J., Moretti, R., Mulligan, V.K., Nerli, S., Norn, C., Ó'Conchúir, S., Ollikainen, N., Ovchinnikov, S., Pacella, M.S., Pan, X., Park, H., Pavlovicz, R.E., Pethe, M., Pierce, B.G., Pilla, K.B., Raveh, B., Renfrew, P.D., Burman, S.S.R., Rubenstein, A., Sauer, M.F., Scheck, A., Schief, W., Schueler-Furman, O., Sedan, Y., Sevy, A.M., Sgourakis, N.G., Shi, L., Siegel, J.B., Silva, D.-A., Smith, S., Song, Y., Stein, A., Szegedy, M., Teets, F.D., Thyme, S.B., Wang, R.Y.-R., Watkins, A., Zimmerman, L., Bonneau, R., 2020. Macromolecular modeling and design in Rosetta: recent methods and frameworks. Nat. Methods. 17 (7), 665-680.

Lenug, D.W., Che, E., Goeddel, D.V., 1989. A method for random mutagenesis of a

1185 defined DNA segment using a modified polymerase chain reaction. Technique JMCMB
1186 1, 11-15.
1187 Levin, S.A., 1992. Mathematics and biology: The interface, challenges and
1188 opportunities.
1189 Linke, J.A., Rayat, A., Ward, J.M., 2023. Production of indigo by recombinant bacteria.
1190 Bioresour. Bioprocess. 10 (1), 20.
1191 Linke, J.A.A., Rayat, A., Ward, J.M.M., 2023. Production of indigo by recombinant
1192 bacteria. Bioresour. Bioprocess. 10 (1), 20.
1193 Lipsh-Sokolik, R., Listov, D., Fleishman, S.J., 2021. The AbDesign computational
1194 pipeline for modular backbone assembly and design of binders and enzymes. Protein
1195 Sci. 30 (1), 151-159.
1196 Liu, H., Chen, Q., 2022. Computational protein design with data-driven approaches:
1197 Recent developments and perspectives. Wiley Interdiscip. Rev.-Comput. Mol. Sci. 13
1198 (3), e1646.
1199 Lončar, N., Fiorentini, F., Bailleul, G., Savino, S., Romero, E., Mattevi, A., Fraaije,
1200 M.W., 2019a. Characterization of a thermostable flavin-containing monooxygenase
1201 from Nitrincola lacisaponensis (NiFMO). Appl. Microbiol. Biotechnol. 103 (4),
1202 1755-1764.
1203 Lončar, N., van Beek, H.L., Fraaije, M.W., 2019b. Structure-based redesign of a
1204 self-sufficient flavin-containing monooxygenase towards indigo production. Int. J. Mol.

1205 Sci. 20 (24), 6148.

1206 Ma, Q., Zhang, X., Qu, Y., 2018. Biodegradation and biotransformation of indole:

1207 advances and perspectives. Front. Microbiol. 9: 2625

1208 Mitsubayashi, K., Hashimoto, Y., 2000. Development of a gas-phase biosensor for

1209 trimethylamine using a flavin-containing monooxygenase 3. Electrochemistry 68 (11),

1210 901-903.

1211 Mitsubayashi, K., Hashimoto, Y., 2002. Bioelectronic nose for methyl mercaptan vapor

1212 using xenobiotic metabolizing enzyme: flavin-containing monooxygenase. Sens.

1213 Actuator B-Chem. 83 (1), 35-40.

1214 Molina-Espeja, P., Garcia-Ruiz, E., Gonzalez-Perez, D., Ullrich, R., Hofrichter, M.,

1215 Alcalde, M., 2014. Directed evolution of unspecific peroxygenase from Agrocybe

1216 aegerita. Appl. Environ. Microbiol. 80 (11), 3496-3507.

1217 Morris, G.M., Huey, R., Lindstrom, W., Sanner, M.F., Belew, R.K., Goodsell, D.S.,

1218 Olson, A.J., 2009. AutoDock4 and AutoDockTools4: Automated docking with selective

1219 receptor flexibility. J. Comput. Chem. 30 (16), 2785-2791.

1220 Murdock, D., Ensley, B.D., Serdar, C., Thalen, M., 1993. Construction of metabolic

1221 operons catalyzing the *de novo* biosynthesis of indigo in *Escherichia coli*. Nat.

1222 Biotechnol. 11 (3), 381-386.

1223 Nicoll, C.R., Bailleul, G., Fiorentini, F., Mascotti, M.L., Fraaije, M.W., Mattevi, A.,

1224 2020. Ancestral-sequence reconstruction unveils the structural basis of function in

mammalian FMOs. Nat. Struct. Mol. Biol. 27 (1), 14-24.

O'Brien, E.J., Lerman, J.A., Chang, R.L., Hyduke, D.R., Palsson, B.Ø., 2013. Genome‐scale models of metabolism and gene expression extend and refine growth phenotype prediction. Mol. Syst. Biol. 9 (1), 693-693.

O'Connor, K.E., Dobson, A., Hartmans, S., 1997. Indigo formation by microorganisms expressing styrene monooxygenase activity. Appl. Environ. Microbiol. 63 (11), 4287-4291.

Orth, J.D., Thiele, I., Palsson, B.Ø., 2010. What is flux balance analysis? Nat. Biotechnol. 28 (3), 245-248.

Pan, Z., Tao, D., Ren, M., Cheng, L., 2023. A combinational optimization method for efficient production of indigo by the recombinant *Escherichia coli* with expression of monooxygenase and malate dehydrogenase. Foods 12 (3), 502.

Pantazes, R.J., Grisewood, M.J., Li, T., Gifford, N.P., Maranas, C.D., 2015. The Iterative Protein Redesign and Optimization (IPRO) suite of programs. J. Comput. Chem. 36 (4), 251-263.

Pathak, H., Madamwar, D., 2010. Biosynthesis of indigo dye by newly isolated naphthalene-degrading strain *Pseudomonas* sp. HOB1 and its application in dyeing cotton fabric. Appl. Biochem. Biotechnol. 160, 1616-1626.

Paul, C.E., Eggerichs, D., Westphal, A.H., Tischler, D., van Berkel, W.J.H., 2021. Flavoprotein monooxygenases: Versatile biocatalysts. Biotechnol. Adv. 51, 107712.

Pazmiño, D.E.T., Snajdrova, R., Rial, D.V., Mihovilovic, M.D., Fraaije, M.W., 2007. Altering the substrate specificity and enantioselectivity of phenylacetone monooxygenase by structure-inspired enzyme redesign. Adv. Synth. Catal. 349 (8-9), 1361-1368.

Peleg, Y., Vincentelli, R., Collins, B.M., Chen, K.-E., Livingstone, E.K., Weeratunga, S., Leneva, N., Guo, Q., Remans, K., Perez, K., Bjerga, G.E.K., Larsen, O., Vanek, O., Skorepa, O., Jacquemin, S., Poterszman, A., Kjaer, S., Christodoulou, E., Albeck, S., Dym, O., Ainbinder, E., Unger, T., Schuetz, A., Matthes, S., Bader, M., de Marco, A., Storici, P., Semrau, M.S., Stolt-Bergner, P., Aigner, C., Suppmann, S., Goldenzweig, A., Fleishman, S.J., 2021. Community-wide experimental evaluation of the PROSS stability-design method. J. Mol. Biol. 433 (13), 166964.

Peng, Z., Wang, W., Wei, H., Li, X., Yang, J., 2023. Improved protein structure prediction with trRosettaX2, AlphaFold2, and optimized MSAs in CASP15. Proteins 1-8.

Pereira, M.S., de Araújo, S.S., Nagem, R.A.P., Richard, J.P., Brandão, T.A.S., 2022. The role of remote flavin adenine dinucleotide pieces in the oxidative decarboxylation catalyzed by salicylate hydroxylase. Bioorg. Chem. 119, 105561.

Phillips, I.R., Shephard, E.A., 2020a. Flavin-containing monooxygenase 3 (FMO3): genetic variants and their consequences for drug metabolism and disease. Xenobiotica 50 (1), 19-33.

Phillips, I.R., Shephard, E.A., 2020b. Flavin-containing monooxygenases: new structures from old proteins. Nat. Struct. Mol. Biol. 27 (1), 3-4.

Polyzos, A.A., 2003. Directed evolution of a sulfoxidation biocatalyst. Dissertation, University of Florida.

Poulsen, L.L., Ziegler, D.M., 1979. The liver microsomal FAD-containing monooxygenase. Spectral characterization and kinetic studies. J. Biol. Chem. 254 (14), 6449-6455.

Qi, Y., Zhang, J.Z.H., 2020. DenseCPD: Improving the accuracy of neural-network-based computational protein sequence design with DenseNet. J. Chem Inf. Model. 60 (3), 1245-1252.

Qi, Y., Zhu, J., Zhang, K., Liu, T., Wang, Y., 2022. Recent development of directed evolution in protein engineering. Syn. Biol. 3 (6), 1081-1108.

Qu, Y., Pi, W., Ma, F., Zhou, J., Zhang, X., 2010. Influence and optimization of growth substrates on indigo formation by a novel isolate Acinetobacter sp. PP-2. Bioresour. Technol. 101 (12), 4527-4532.

Qu, Y., Shi, S., Zhou, H., Ma, Q., Li, X., Zhang, X., Zhou, J., 2012a. Characterization of a novel phenol hydroxylase in indoles biotranformation from a strain *Arthrobacter* sp. W1.

Qu, Y., Zhang, X., Ma, Q., Ma, F., Zhang, Q., Li, X., Zhou, H., Zhou, J., 2012b. Indigo biosynthesis by Comamonas sp. MQ. Biotechnol. Lett. 34 (2), 353-357.

1285 Rackers, J.A., Wang, Z., Lu, C., Laury, M.L., Lagardere, L., Schnieders, M.J., Piquemal,
1286 J.P., Ren, P.Y., Ponder, J.W., 2018. Tinker 8: Software tools for molecular design. J.
1287 Chem. Theory Comput. 14 (10), 5273-5289.
1288 Ramana, P., Herman, W., Hiroux, C., Adams, E., Augustijns, P., Van Schepdael, A.,
1289 2017. Evaluation of immobilized $hFMO_3$ on magnetic nanoparticles by capillary zone
1290 electrophoresis. Bioanalysis 9 (3), 289-296.
1291 Ravi, S., Gunawan, R., 2021. ΔFBA—Predicting metabolic flux alterations using
1292 genome-scale metabolic models and differential transcriptomic data. PLoS Comput.
1293 Biol. 17 (11), e1009589.
1294 Riebel, A., de Gonzalo, G., Fraaije, M.W., 2013. Expanding the biocatalytic toolbox of
1295 flavoprotein monooxygenases from *Rhodococcus jostii* RHA1. J. Mol. Catal. B: Enzym.
1296 88, 20-25.
1297 Rioz-Martinez, A., Kopacz, M., de Gonzalo, G., Torres Pazmino, D.E., Gotor, V.,
1298 Fraaije, M.W., 2011. Exploring the biocatalytic scope of a bacterial flavin-containing
1299 monooxygenase. Org. Biomol. Chem. 9 (5), 1337-1341.
1300 Sabourin, P.J., Hodgson, E., 1984. Characterization of the purified microsomal
1301 FAD-containing monooxygenase from mouse and pig liver. Chem. Biol. Interact. 51 (2),
1302 125-139.
1303 Sadeghi, S.J., Fantuzzi, A., Gilardi, G., 2011. Breakthrough in P450 bioelectrochemistry
1304 and future perspectives. Biochim. Biophys. Acta 1814 (1), 237-248.

1305 Sadeghi, S.J., Meirinhos, R., Catucci, G., Dodhia, V.R., Nardo, G.D., Gilardi, G., 2010.
1306 Direct electrochemistry of drug metabolizing human flavin-containing monooxygenase:
1307 Electrochemical turnover of benzydamine and tamoxifen. J. Am. Chem. Soc. 132 (2),
1308 458-459.
1309 Saito, H., Shirai, T., Kudo, H., Mitsubayashi, K., 2008. Electrochemical sensor with
1310 flavin-containing monooxygenase for triethylamine solution. Anal. Bioanal. Chem. 391
1311 (4), 1263-1268.
1312 Schmidt, A.C., Leroux, J.C., 2020. Treatments of trimethylaminuria: where we are and
1313 where we might be heading. Drug Discov. Today 25 (9), 1710-1717.
1314 Schnepel, C., Dodero, V.I., Sewald, N., 2021. Novel arylindigoids by late-stage
1315 derivatization of biocatalytically synthesized dibromoindigo. Chem. 27 (17),
1316 5404-5411.
1317 Senthong, V., Wang, Z., Fan, Y., Wu, Y., Hazen, S.L., Tang, W.H., 2016. Trimethylamine
1318 N-oxide and mortality risk in patients with peripheral artery disease. J. Am. Heart.
1319 Assoc. 5 (10), e004237.
1320 Shao, Z., Zhao, H., Giver, L., Arnold, F.H., 1998. Random-priming in vitro
1321 recombination: An effective tool for directed evolution. Nucleic Acids Res. 26 (2),
1322 681-683.
1323 Shehin-Johnson, S.E., Williams, D.E., Larsen-Su, S., Stresser, D.M., Hines, R.N., 1995.
1324 Tissue-specific expression of flavin-containing monooxygenase (FMO) forms 1 and 2 in

the rabbit. J. Pharmacol. Exp. Ther. 272 (3), 1293-1299.

Shimada, A., Fujii, N., Saito, T., 2004. Chapter 26 - Tryptophanase Activity on D-Tryptophan, in: Pályi, G., Zucchi, C., Caglioti, L. (Eds.), Progress in Biological Chirality. Elsevier Science Ltd, Oxford, pp. 321-327.

Siddiqui, J.K., Baskin, E., Liu, M., Cantemir-Stone, C.Z., Zhang, B., Bonneville, R., McElroy, J.P., Coombes, K.R., Mathé, E.A., 2018. IntLIM: integration using linear models of metabolomics and gene expression data. BMC Bioinform. 19 (1), 81.

Sieber, V., Martinez, C.A., Arnold, F.H., 2001. Libraries of hybrid proteins from distantly related sequences. Nat. Biotechnol. 19 (5), 456-460.

Singh, A., Singh Chauhan, N., Thulasiram, H.V., Taneja, V., Sharma, R., 2010. Identification of two flavin monooxygenases from an effluent treatment plant sludge metagenomic library. Bioresour. Technol. 101 (21), 8481-8484.

Søndergaard, C.R., Olsson, M.H.M., Rostkowski, M., Jensen, J.H., 2011. Improved treatment of ligands and coupling effects in empirical calculation and rationalization of pka values. J. Chem. Theory Comput. 7 (7), 2284-2295.

Stasiak, N., Kukuła-Koch, W., Głowniak, K., 2014. Modern industrial and pharmacological applications of indigo dye and its derivatives--a review. Acta Pol. Pharm. 71 (2), 215-221.

Stephens, G.M., Sidebotham, J.M., Mann, N.H., Dalton, H., 1989. Cloning and expression in *Escherichia coli* of the toluene dioxygenase gene from *Pseudomonas*

putida NCIB11767. FEMS Microbiol. Lett. 57 (3), 295-300.

Suh, J.-K., Poulsen, L.L., Ziegler, D.M., Robertus, J.D., 1996. Molecular cloning and kinetic characterization of a flavin-containing monooxygenase from *Saccharomyces cerevisiae*. Arch. Biochem. Biophys. 336 (2), 268-274.

Suh, J.K., Poulsen, L.L., Ziegler, D.M., Robertus, J.D., 1999. Yeast flavin-containing monooxygenase generates oxidizing equivalents that control protein folding in the endoplasmic reticulum. PNAS 96 (6), 2687-2691.

Sun, B.Y., Sui, H.L., Liu, Z.W., Tao, X.Y., Gao, B., Zhao, M., Ma, Y.S., Zhao, J., Liu, M., Wang, F.Q., Wei, D.Z., 2022. Structure-guided engineering of a flavin-containing monooxygenase for the efficient production of indirubin. Bioresour. Bioprocess. 9 (1), 70.

Tan, C., Zhang, X., Zhu, Z., Xu, M., Yang, T., Osire, T., Yang, S., Rao, Z., 2019. Asp305Gly mutation improved the activity and stability of the styrene monooxygenase for efficient epoxide production in *Pseudomonas putida* KT2440. Microb. Cell Fact. 18 (1), 12.

Tang, W.H.W., Bäckhed, F., Landmesser, U., Hazen, S.L., 2019. Intestinal microbiota in cardiovascular health and disease: JACC state-of-the-art review. J. Am. Coll. Cardiol. 73 (16), 2089-2105.

Taylor, K.L., Ziegler, D., 1987. Studies on substrate specificity of the hog liver flavin-containing monooxygenase: anionic organic sulfur compounds. Biochem.

1365 Pharmacol. 36 (1), 141-146.

1366 Thiele, I., Palsson, B.Ø., 2010. A protocol for generating a high-quality genome-scale
1367 metabolic reconstruction. Nat. Protoc. 5 (1), 93-121.

1368 Treacy, E.P., Akerman, B.R., Chow, L.M., Youil, R., Bibeau, C., Lin, J., Bruce, A.G.,
1369 Knight, M., Danks, D.M., Cashman, J.R., Forrest, S.M., 1998. Mutations of the
1370 flavin-containing monooxygenase gene (FMO3) cause trimethylaminuria, a defect in
1371 detoxication. Hum. Mol. Genet. 7 (5), 839-845.

1372 Tsuji, T., Onimaru, M., Yanagawa, H., 2001. Random multi-recombinant PCR for the
1373 construction of combinatorial protein libraries. Nucleic Acids Res. 29 (20), e97.

1374 Tynes, R.E., Sabourin, P.J., Hodgson, E., 1985. Identification of distinct hepatic and
1375 pulmonary forms of microsomal flavin-containing monooxygenase in the mouse and
1376 rabbit. Biochem. Biophys. Res. Commun. 126 (3), 1069-1075.

1377 Tynes, R.E., Sabourin, P.J., Hodgson, E., Philpot, R.M., 1986. Formation of hydrogen
1378 peroxide and N-hydroxylated amines catalyzed by pulmonary flavin-containing
1379 monooxygenases in the presence of primary alkylamines. Arch. Biochem. Biophys. 251
1380 (2), 654-664.

1381 Uno, Y., Shimizu, M., Yamazaki, H., 2013. Molecular and functional characterization of
1382 flavin-containing monooxygenases in cynomolgus macaque. Biochem. Pharmacol. 85
1383 (12), 1837-1847.

1384 Valentino, H., Campbell, A.C., Schuermann, J.P., Sultana, N., Nam, H.G., LeBlanc, S.,

Tanner, J.J., Sobrado, P., 2020. Structure and function of a flavin-dependent S-monooxygenase from garlic (Allium sativum). J. Biol. Chem. 295 (32), 11042-11055.

van Berkel, W.J.H., Kamerbeek, N.M., Fraaije, M.W., 2006. Flavoprotein monooxygenases, a diverse class of oxidative biocatalysts. J. Biotechnol. 124 (4), 670-689.

Wang, J., Lisanza, S., Juergens, D., Tischer, D., Watson, J.L., Castro, K.M., Ragotte, R., Saragovi, A., Milles, L.F., Baek, M., Anishchenko, I., Yang, W., Hicks, D.R., Exposit, M., Schlichthaerle, T., Chun, J.H., Dauparas, J., Bennett, N., Wicky, B.I.M., Muenks, A., DiMaio, F., Correia, B., Ovchinnikov, S., Baker, D., 2022. Scaffolding protein functional sites using deep learning. Science 377 (6604), 387-394.

Wang, X., Xu, K., Tan, Y., Liu, S., Zhou, J., 2023. Possibilities of Using De Novo Design for Generating Diverse Functional Food Enzymes. Int. J. Mol. Sci. 24 (4), 3827.

Wani, K.A., Goswamy, D., Taubert, S., Ratnappan, R., Ghazi, A., Irazoqui, J.E., 2021. NHR-49/PPAR-alpha and HLH-30/TFEB cooperate for *C. elegans* host defense via a flavin-containing monooxygenase. Elife 10, e62775.

Watson, J.L., Juergens, D., Bennett, N.R., Trippe, B.L., Yim, J., Eisenach, H.E., Ahern, W., Borst, A.J., Ragotte, R.J., Milles, L.F., Wicky, B.I.M., Hanikel, N., Pellock, S.J., Courbet, A., Sheffler, W., Wang, J., Venkatesh, P., Sappington, I., Torres, S.V., Lauko, A., De Bortoli, V., Mathieu, E., Ovchinnikov, S., Barzilay, R., Jaakkola, T.S., DiMaio, F., Baek, M., Baker, D., 2023. *De novo* design of protein structure and function with

RFdiffusion. Nature 620 (7976), 1089-1100.

Weissenow, K., Heinzinger, M., Rost, B., 2022. Protein language-model embeddings for fast, accurate, and alignment-free protein structure prediction. Structure 30 (8), 1169-1177.e4.

Wicky, B.I.M., Milles, L.F., Courbet, A., Ragotte, R.J., Dauparas, J., Kinfu, E., Tipps, S., Kibler, R.D., Baek, M., DiMaio, F., Li, X., Carter, L., Kang, A., Nguyen, H., Bera, A.K., Baker, D., 2022. Hallucinating symmetric protein assemblies. Science 378 (6615), 56-61.

Wijma, H.J., Furst, M.J.L.J., Janssen, D.B., 2018. A Computational Library Design Protocol for Rapid Improvement of Protein Stability: FRESCO, in: Bornscheuer, U.T., Hohne, M. (Eds.), Protein Engineering:Methods and Protocols. Humana New York, New York, pp. 69-85.

Wojaczyńska, E., Wojaczyński, J., 2020. Modern stereoselective synthesis of chiral sulfinyl compounds. Chem. Rev. 120 (10), 4578-4611.

Woo, H.-j., Sanseverino, J., Cox, C.D., Robinson, K.G., Sayler, G.S., 2000. The measurement of toluene dioxygenase activity in biofilm culture of *Pseudomonas putida* F1. J. Microbiol. Methods. 40 (2), 181-191.

Wood, C.W., Heal, J.W., Thomson, A.R., Bartlett, G.J., Ibarra, A.A., Brady, R.L., Sessions, R.B., Woolfson, D.N., 2017. ISAMBARD: an open-source computational environment for biomolecular analysis, modelling and design. Bioinformatics 33 (19),

3043-3050.

Woolfson, D.N., 2021. A brief history of *de novo* protein design: Minimal, rational, and computational. J. Mol. Biol. 433 (20), 167160.

Wyatt, M.K., Overby, L.H., Lawton, M.P., Philpot, R.M., 1998. Identification of amino acid residues associated with modulation of flavin-containing monooxygenase (FMO) activity by imipramine: Structure/function studies with FMO1 from pig and rabbit. Biochemistry 37 (17), 5930-5938.

Xiong, P., Chen, Q., Liu, H., 2017. Computational Protein Design Under a Given Backbone Structure with the ABACUS Statistical Energy Function, in: Samish, I. (Ed.) Computational Protein Design. Springer New York, New York, pp. 217-226.

Xiong, W., Liu, B., Shen, Y., Jing, K., Savage, T.R., 2021. Protein engineering design from directed evolution to de novo synthesis. Biochem. Eng. J. 174, 108096.

Xu, J., Yang, Y., 2021. Gut microbiome and its meta-omics perspectives: profound implications for cardiovascular diseases. Gut Microbes 13 (1), 1936379.

Yang, J.E., Park, S.J., Kim, W.J., Kim, H.J., Kim, B.J., Lee, H., Shin, J., Lee, S.Y., 2018. One-step fermentative production of aromatic polyesters from glucose by metabolically engineered Escherichia coli strains. Nat. Commun. 9 (1), 79.

Yang, L., Li, X., Huang, W., Rao, X., Lai, Y., 2022. Pharmacological properties of indirubin and its derivatives. Biomed. Pharmacother. 151, 113112.

Yang, S., Li, X., Yang, F., Zhao, R., Pan, X., Liang, J., Tian, L., Li, X., Liu, L., Xing, Y.,

Wu, M., 2019. Gut microbiota-dependent marker tmao in promoting cardiovascular disease: Inflammation mechanism, clinical prognostic, and potential as a therapeutic target. Front. Pharmacol. 10, 1360.

YANG Ya-kun, S.L., LI Yan, 2017. Role of FMOs in drug metabolism and development. Acta Pharm. Sin. 52 (10), 1485-1495.

Yang, Z., Zeng, X., Zhao, Y., Chen, R., 2023. AlphaFold2 and its applications in the fields of biology and medicine. Signal Transduct. Target. Ther. 8 (1), 115.

Yeh, A.H.-W., Norn, C., Kipnis, Y., Tischer, D., Pellock, S.J., Evans, D., Ma, P., Lee, G.R., Zhang, J.Z., Anishchenko, I., Coventry, B., Cao, L., Dauparas, J., Halabiya, S., DeWitt, M., Carter, L., Houk, K.N., Baker, D., 2023. *De novo* design of luciferases using deep learning. Nature 614 (7949), 774-780.

Yim, H., Haselbeck, R., Niu, W., Pujol-Baxley, C., Burgard, A., Boldt, J., Khandurina, J., Trawick, J.D., Osterhout, R.E., Stephen, R., Estadilla, J., Teisan, S., Schreyer, H.B., Andrae, S., Yang, T.H., Lee, S.Y., Burk, M.J., Dien, S.V., 2011. Metabolic engineering of Escherichia coli for direct production of 1,4-butanediol. Nat. Chem. Biol. 7 (7), 445-452.

Yizhak, K., Benyamini, T., Liebermeister, W., Ruppin, E., Shlomi, T., 2010. Integrating quantitative proteomics and metabolomics with a genome-scale metabolic network model. Bioinformatics 26 (12), i255-i260.

Zane, N.R., Chen, Y., Wang, M.Z., Thakker, D.R., 2018. Cytochrome P450 and

flavin-containing monooxygenase families: age-dependent differences in expression and functional activity. Pediatr. Res. 83 (2), 527-535.

Zhang, J., Cashman, J.R., 2006. Quantitative analysis of FMO gene mRNA levels in human tissues. Drug Metab. Dispos. 34 (1), 19-26.

Zhang, Y., Wu, Y.-Q., Xu, N., Zhao, Q., Yu, H.-L., Xu, J.-H., 2019. Engineering of cyclohexanone monooxygenase for the enantioselective synthesis of (S)-omeprazole. ACS Sustain. Chem. Eng. 7 (7), 7218-7226.

Zhao, H., Giver, L., Shao, Z., Affholter, J.A., Arnold, F.H., 1998. Molecular evolution by staggered extension process (StEP) *in vitro* recombination. Nat. Biotechnol. 16 (3), 258-261.

Zheng, W., Li, Y., Zhang, C., Zhou, X., Pearce, R., Bell, E.W., Huang, X., Zhang, Y., 2021. Protein structure prediction using deep learning distance and hydrogen-bonding restraints in CASP14. Proteins 89 (12), 1734-1751.

Zhu, W., Buffa, J.A., Wang, Z., Warrier, M., Schugar, R., Shih, D.M., Gupta, N., Gregory, J.C., Org, E., Fu, X., Li, L., DiDonato, J.A., Lusis, A.J., Brown, J.M., Hazen, S.L., 2018. Flavin monooxygenase 3, the host hepatic enzyme in the metaorganismal trimethylamine N-oxide-generating pathway, modulates platelet responsiveness and thrombosis risk. J. Thromb. Haemost. 16 (9), 1857-1872.

Ziegler, D.M., 1993. Recent studies on the structure and function of multisubstrate flavin-containing monooxygenases. Annu. Rev. Pharmacol. Toxicol. 33, 179-199.

1485 Ziegler, D.M., 2002. An overview of the mechanism, substrate specificities, and
1486 structure of FMOs. Drug Metab. Rev. 34 (3), 503-511.
1487 Ziegler, D.M., Mitchell, C.H., 1972. Microsomal oxidase IV: Properties of a
1488 mixed-function amine oxidase isolated from pig liver microsomes. Arch. Biochem.
1489 Biophys. 150 (1), 116-125.
1490 [dataset] Fan, C., Xie, Z., 2023. AutoDock Docking Results between mFMO and Indole.
1491 Mendeley Data, v1. https://doi.org/10.17632/zrmhyr5y32.1.

Graphic Abstract

Click here to access/download;Figure;Graphic Abstract.tif

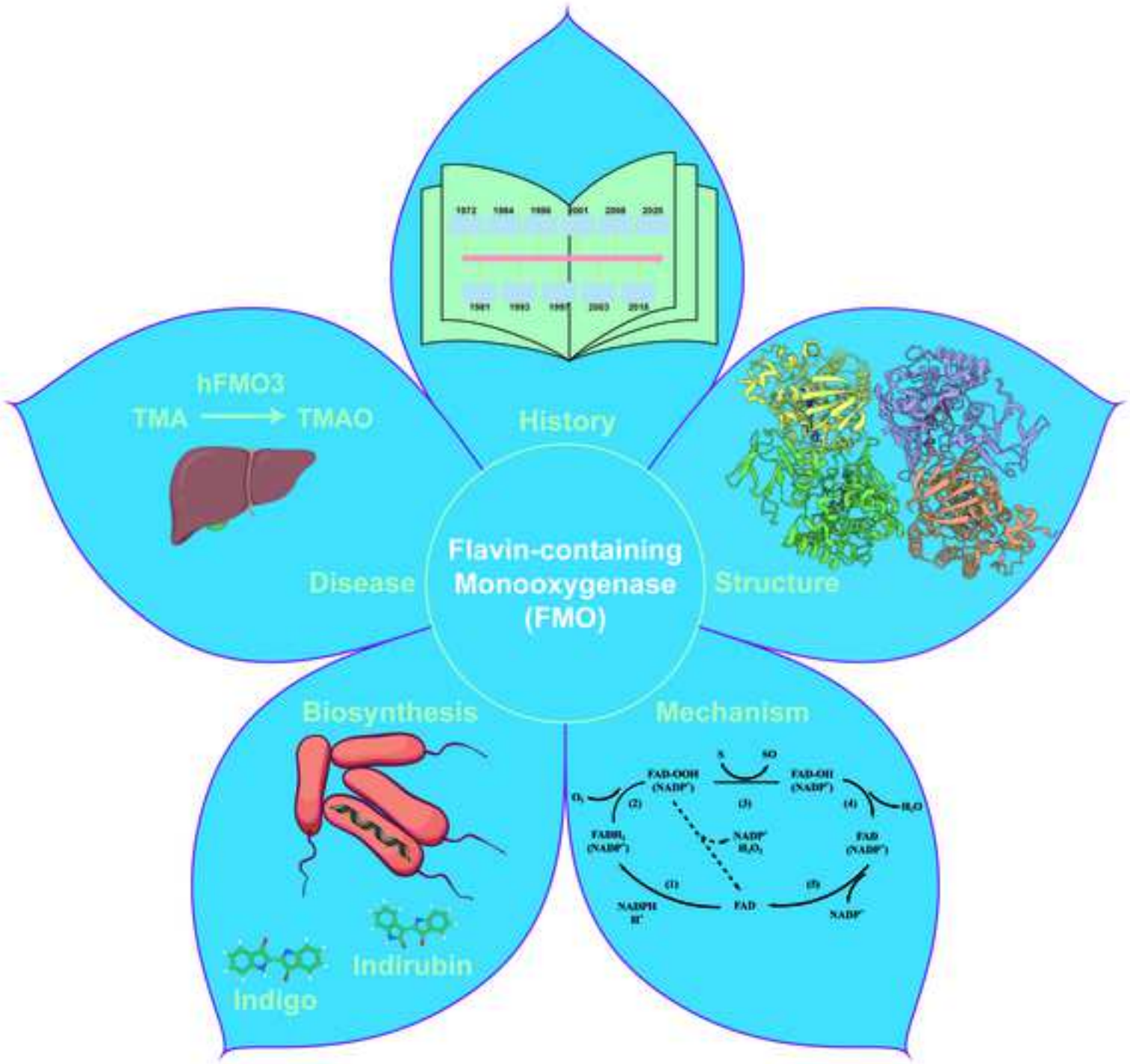

Captions

Figure 1. The timeline of research history about FMO and its application to indigo biosynthesis (A) Crucial time points in the research history of FMO (B) Crucial time points in indigo biosynthesis with FMO.

Figure 2. Sequence alignments of FMOs across various species. (A) The consensus sequences of *Homo sapiens* FMO3 (hFMO), *ancient mammalian* FMO (ancFMO3-6), *Methylophaga* sp. strain SK1 FMO (mFMO), *Schizosaccharomyces pombe* FMO (spFMO), *Corynebacterium glutamicum* FMO (cFMO), and *Nitrincola lacisaponensis* FMO (NiFMO) were identified. The putative FAD, FMO-identifying motif, and NADPH pyrophosphate binding domain are colored blue. Some active sites are colored with ClustalX. The alignment was performed with ClustalW, Jalview, and ESPript (B) Protein sequence identity (%) between different FMOs.

Figure 3. The structure of AncFMO3-6. (A) The cartoon of homo-dimer AncFMO3-6 (PDB ID: 6se3.1) is exhibited from the front perspective. Pale cyan: Rossmann fold for FAD, 2-154 AA (Amino acids), 331-442 AA. Light blue: Rossmann fold for NADP(H), 155-213 AA, 296-330 AA. Orange: the ridged triangular fold, 214-295 AA. Green: 443-507 AA. Pale green: 510-532 AA. Pale yellow: FAD. Light pink: NADP(H). Red: oxygen; (B) The ridged triangular fold and the catalytic cavity are exhibited from the front perspective. The black arrow points to the catalytic cavity; (C) The tunnel is exhibited from the bottom perspective (left) and upper perspective (right). The black dotted line means the connected surface of homo-dimer AncFMO3-6. The black arrows point to the tunnel and the catalytic cavity; (D) The

mesh of amino acids which form hydrogen bonds with NADP(H) and FAD; (E) The amino acids (S13, E32, R33, L40, W41, R51, T60, N61, S62, V110, and T378) form hydrogen bonds with FAD; (F) The amino acids (F59, N61, L192, N194, S195, S216, E281, and Q373) form hydrogen bonds with NADP(H).

Figure 4. The structure and catalytic mechanism of mFMO. (A) The cartoon of homo-dimer mFMO (PDB ID: 2vq7) is exhibited from the front perspective. Pale cyan: Rossmann fold for FAD, 1-169 AA and 281-461 AA. Light blue: Rossmann fold for NADP(H), 170-280 AA. Pale yellow: FAD. Light pink: NADP(H). Pale green: three loops, 44-80 AA, 166-186 AA, and 276-306 AA; (B) The catalytic cavity is exhibited from the front perspective. The black arrow points to the catalytic cavity; (C) The three loops are exhibited linking the binding domains of NADP(H) and FAD; (D) Y212 protects the catalytic cavity from the solvents (E) The catalytic mechanism of FMOs. The sulfur atom is regarded as the substrate.

Figure 5. The docking result of indole and mFMO via AutoDock. (A) The cartoon of mFMO (PDB ID: 2vq7) with indole (Compound CID: 798) is exhibited from the front perspective. Pale cyan: Rossmann fold for FAD, 1-169 AA and 281-461 AA. Light blue: Rossmann fold for NADP(H), 170-280 AA. Pale yellow: FAD. Light pink: NADP(H). Pale green: three loops, 44-80 AA, 166-186 AA, and 276-306 AA. Green sticks: indole. Yellow dotted line: hydrogen bonds; (B) The surface model of mFMO with indole. Light blue dots: Tyr212 (C) The mechanism of indigo biosynthesis.

Figure 6. The sketch map of directed evolution to improve indigo biosynthesis via FMOs.

Figure 7. Demonstrations of some *de novo* design methods. (A) Active center design for enzymes and protein binders; (B) Sketch maps of some AI-based tools for protein scaffold design, including hallucination, inpainting, and MPNN; (C) Validation techniques for *de novo* design proteins.

Figure 8. Various methods of FMOs immobilization. (A) FMOs were adsorbed by support materials; (B) FMOs formed covalent bonds with support materials; (C) FMOs were cross-linked by a cross-linking agent; (D) FMOs were entrapped within a polymeric network; (E) FMOs were enclosed in a spherical semipermeable membrane; (F) FMOs were immobilized on graphene oxide (GO). Didodecyldimethylammonium bromide (DDAB) played as an interface between GO and FMOs. FMOs-DDAB-GO was on glassy carbon (GC) electrodes.

Figure 9. Metabolic and fermentation engineering to improve biosynthesis of FMOs. (A) A suitable chassis should be chosen for further improvements; (B) The establishment and application of genome-scale metabolic network models (GEMs); (C) Optimization in fermentation engineering to increase the production of indigo biosynthesis.

Figure 1

Click here to access/download;Figure;Overview of FMO_Figure 1.tif

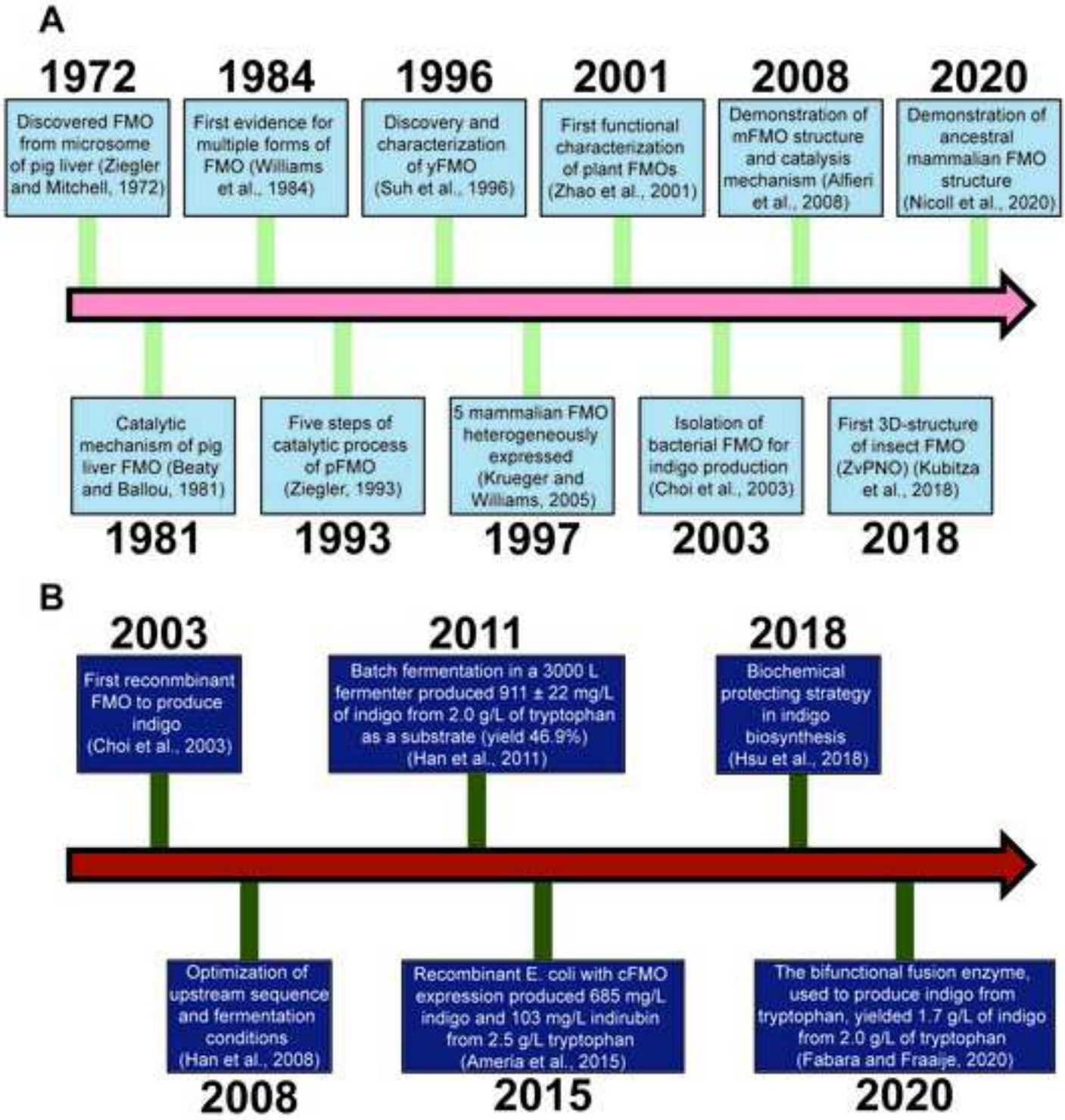

Figure 2

Click here to access/download;Figure;Overview of FMO_Figure 2.tif

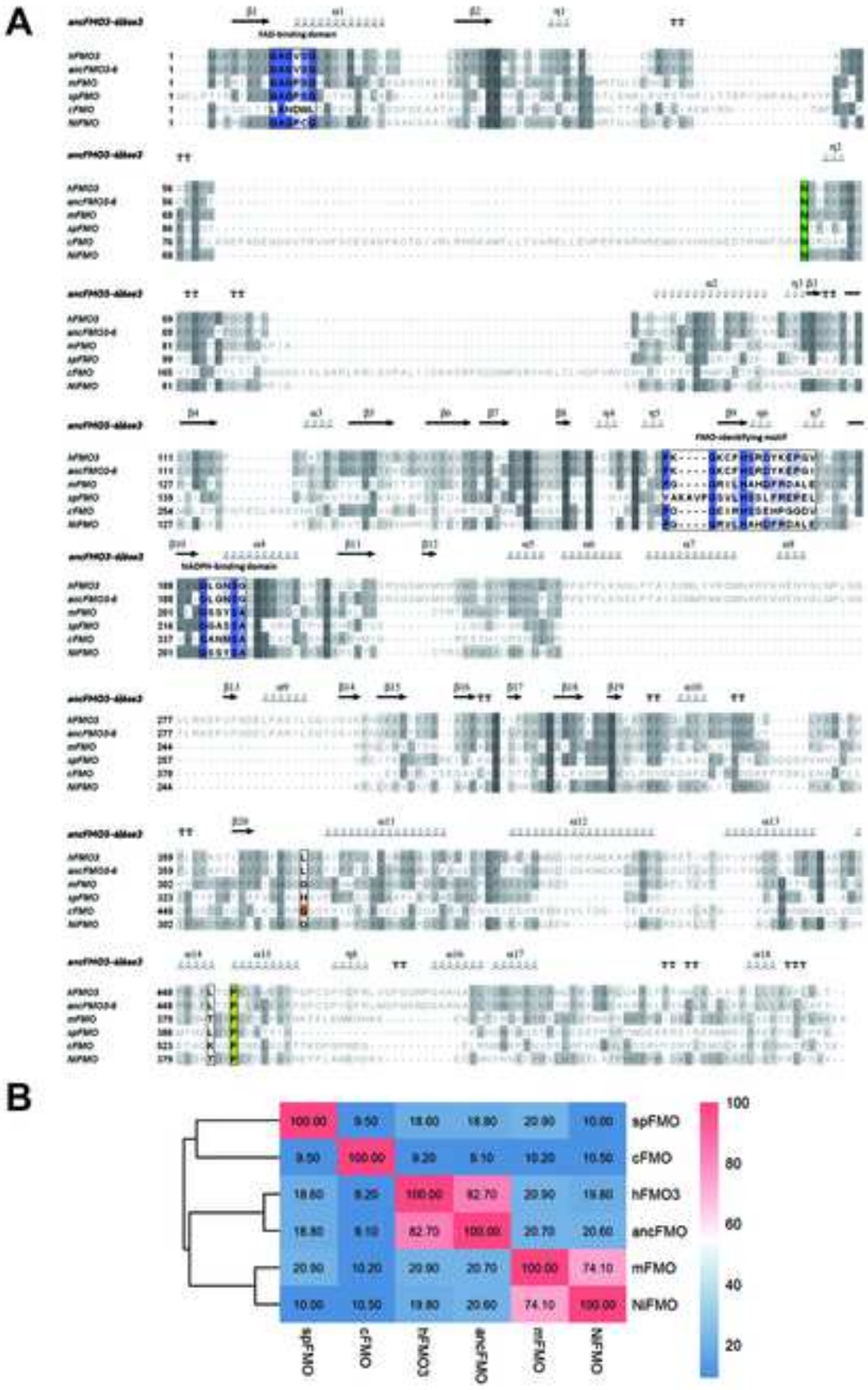

Figure 3

Click here to access/download;Figure;Overview of FMO_Figure 3.tif

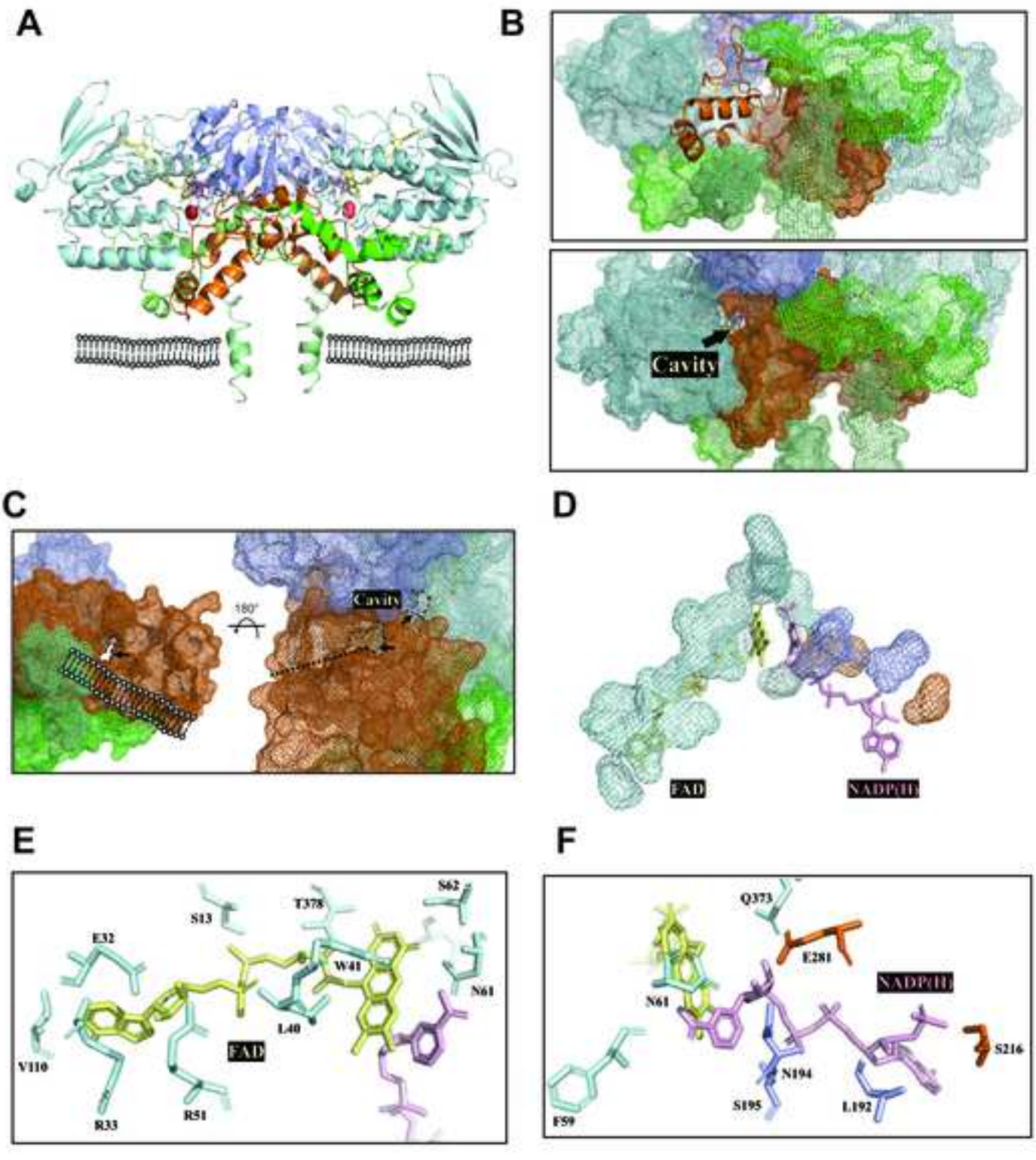

Figure 4

Click here to access/download;Figure;Overview of FMO_Figure 4.tif

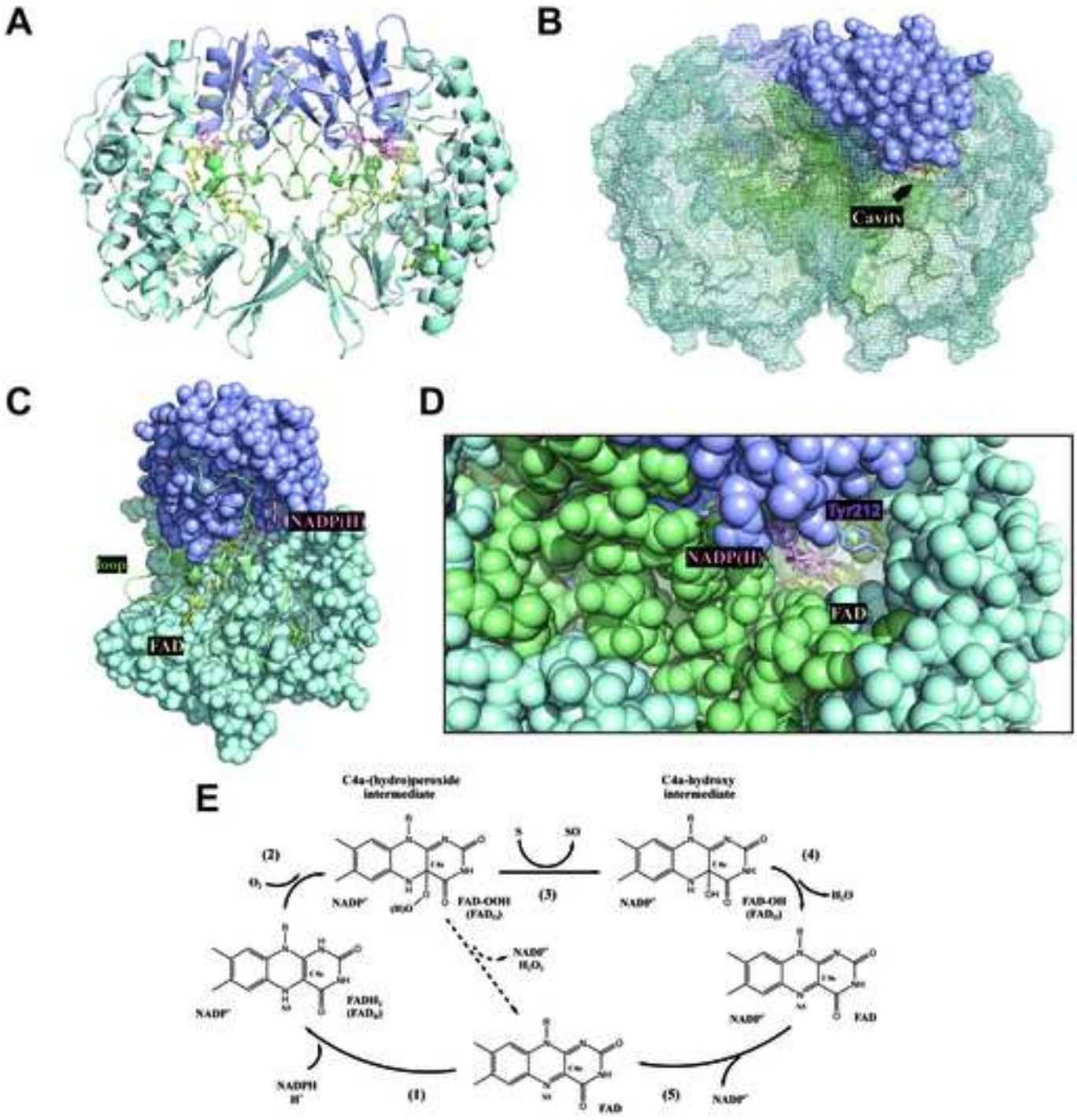

Figure 5

Click here to access/download;Figure;Overview of FMO_Figure 5.tif

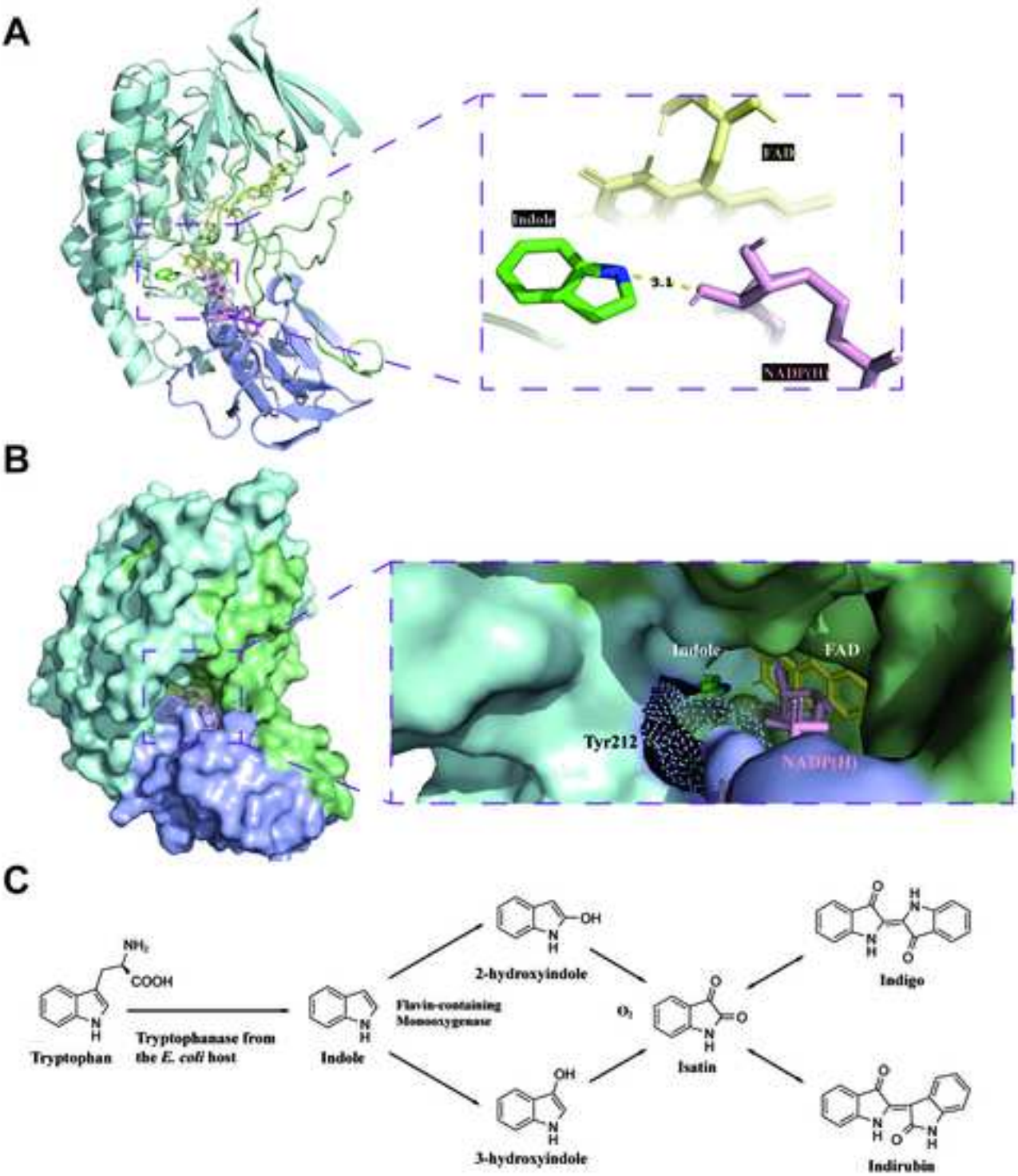

Figure 6

Click here to access/download;Figure;Overview of FMO_Figure 6.tif

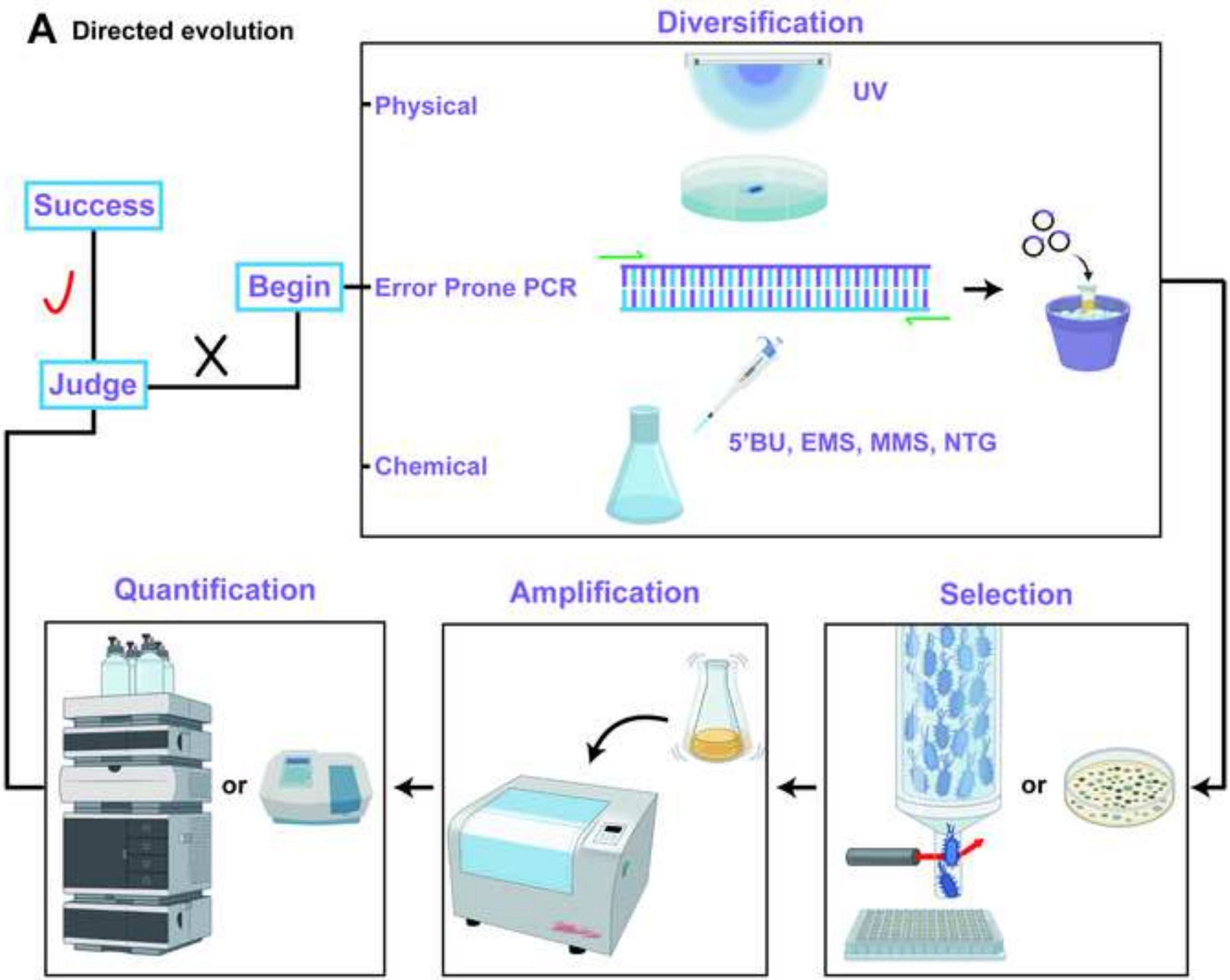

Figure 7

Click here to access/download;Figure;Overview of FMO_Figure 7.tif

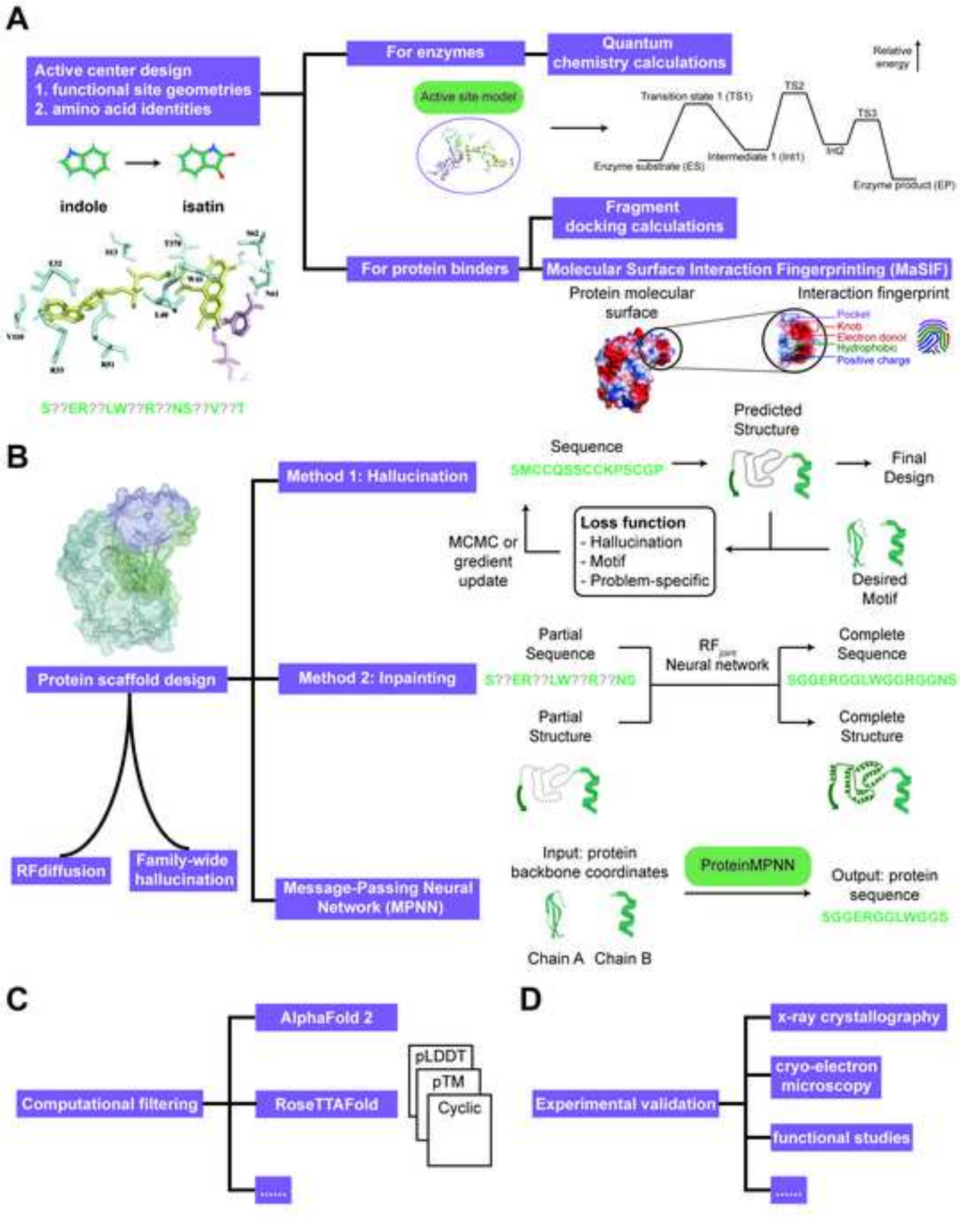

Figure 8

Click here to access/download;Figure;Overview of FMO_Figure 8.tif

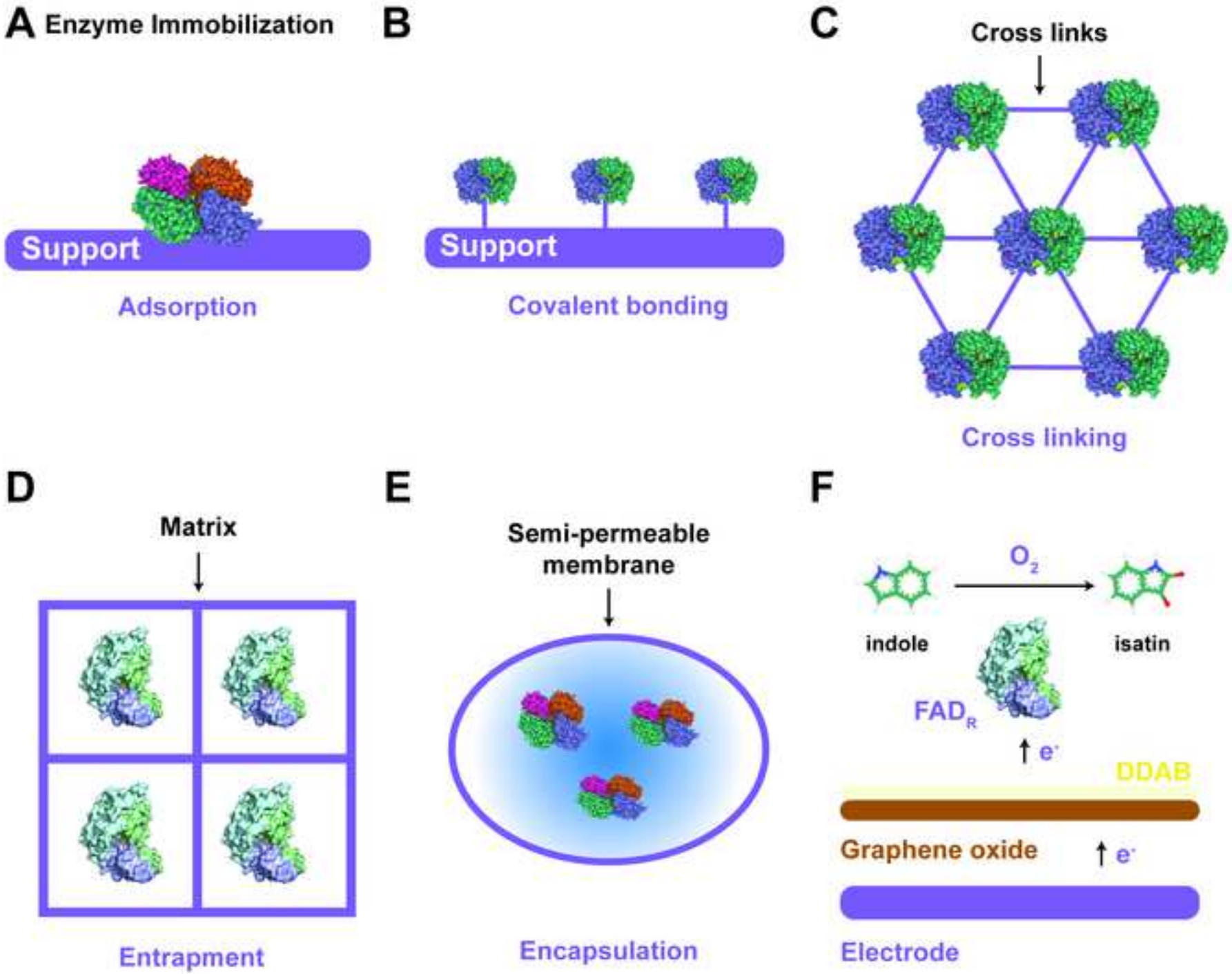

Figure 9

Click here to access/download;Figure;Overview of FMO_Figure 9.tif

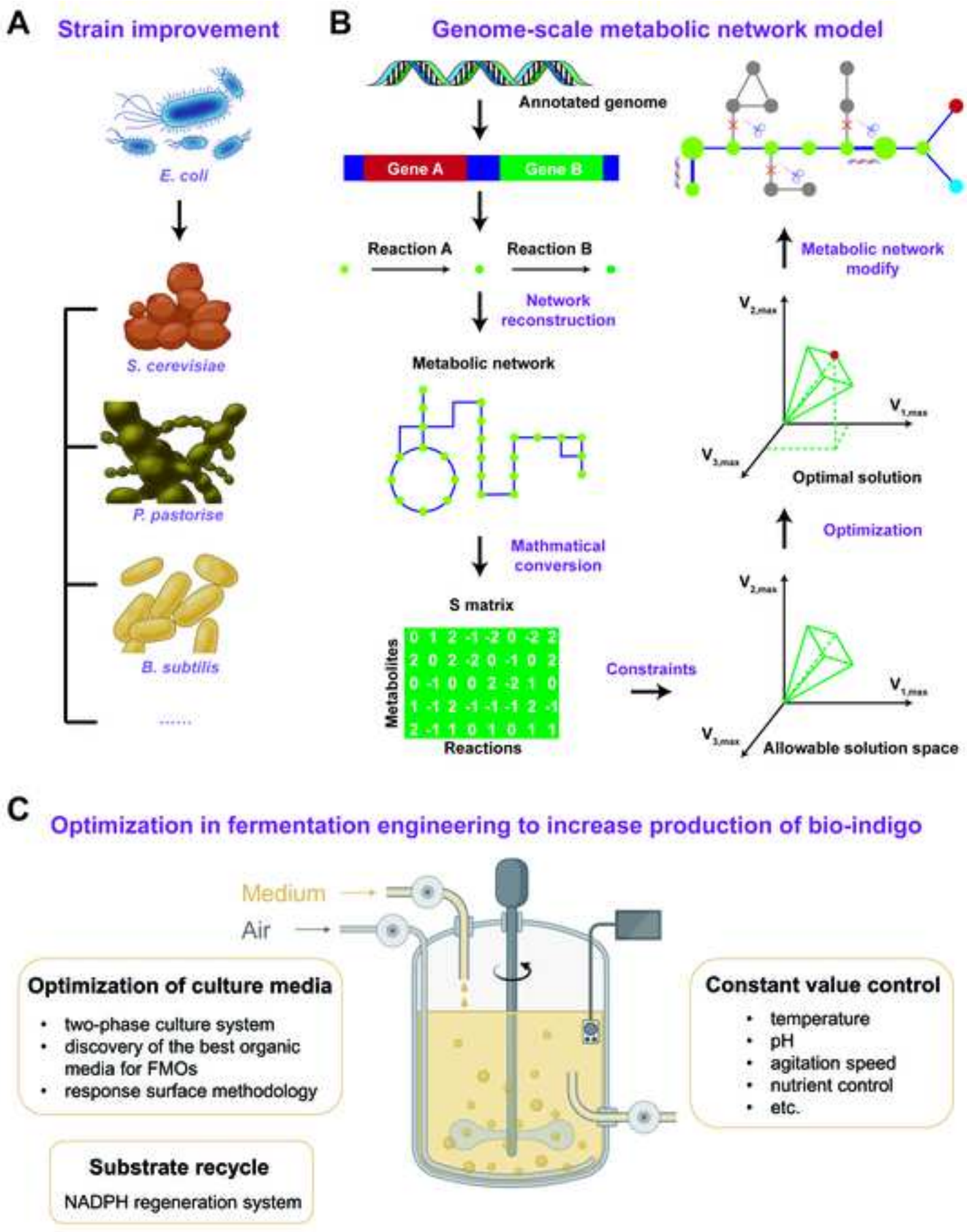

Click here to access/download
Data Statement
Data statement.docx